contributing factors enhancing oncogenesis and the growth and metastasis of prostate cancer. There is also growing evidence that omega-6 (ω-6) polyunsaturated fatty acids (PUFAs) promote prostate cancer growth, whereas ω-3 PUFA, from marine foods, are inhibitory (Rose, 1997; Larsson *et al.*, 2004; Leitzmann *et al.*, 2004), and high blood levels of ω-3 PUFA are associated with a reduced risk of prostate cancer (Chavarro *et al.*, 2007). Thus, excessive amounts of ω-6 PUFAs and a higher ratio of ω-6/ω-3 PUFAs in prostate cells may contribute to an increased incidence of prostate cancer. Consequently, increasing dietary ω-3 PUFAs, such as eicosapentaenoic acid (EPA), and decreasing the ω-6/ω-3 ratios of prostate cells appears to be a feasible approach to reduce the risk and control growth of prostate cancer an of its metastasis, resulting in increased survival (Larsson *et al.*, 2004; Kelavkar *et al.*, 2006; Chavarro *et al.*, 2007). However, the basic mechanisms underlying these protective effects of EPA remain undefined.

Ion channels play essential roles in cell function, that is, cell growth, metastasis and secretion in many types of cells, including cancer cells. EPA has been reported to modulate membrane-bound proteins such as ion channels, that is, voltage-gated Ca^{2+} channels (Xiao *et al.*, 1997) and voltage-gated Na^+ channels (Na_v) (Xiao *et al.*, 1995; 1998; Kang and Leaf, 1996; Jo *et al.*, 2005). The binding sites of EPA on Na_v have been proposed to be located on the cytoplasmic segment of the Na^+ channel, in the α-subunit linking transmembrane repeats III and IV (Xiao *et al.*, 2001). Thus, Na_v appears to be an important target protein for EPA. A number of papers have reported that the up-regulation of the current (I_{Na}) carried by Na_v channels is observed in malignant tumours of prostate, as compared with non-malignant tumours, and contributes to the progression and metastasis by enhancing a number of metastatic cell functions such as invasion, secretion and endocytosis (Grimes *et al.*, 1995; Fraser *et al.*, 2000; 2003; Anderson *et al.*, 2003; Bennett *et al.*, 2004; Krasowska *et al.*, 2004; Brackenbury and Djamgoz, 2006). So far, 10 types of α-subunit in Na channels, referred to as SCN1A to SCN11A, have been identified (Goldin, 1999; 2002; nomenclature follows Alexander *et al.*, 2008). The protein $Na_v1.7$ encoded by the SCN9A gene has been reported to a major carrier of the functional I_{Na} expressed in prostate cancer cells (Diss *et al.*, 2001; 2005). However, the effects of EPA on I_{Na} in prostate cancer cells have not been investigated.

To elucidate the protective effects of EPA on prostate cancer, the effects of EPA on I_{Na} were examined by the whole-cell patch-clamp technique and effects on the Na_v transcripts by real-time reverse transcriptase polymerase chain reaction (RT-PCR) analysis, in human and rat prostate cancer cells (PC-3 and Mat-LyLu cell lines). The alterations in fatty acid composition of cellular phospholipids after treatment with EPA and functions of prostate cancer cells contributing to metastasis (proliferation, invasion and endocytosis) were also investigated.

Methods

Cell preparation

PC-3 human prostate epithelial tumour cell lines and Mat-LyLu rat epithelial tumour cell lines were obtained from JCRB cell bank (Osaka, Japan) and European Collection of Cell Cultures (ECACC, Wiltshire, UK) respectively. PC-3 cells were grown in Kaighn's modification of Ham's F12 medium (F12K) with 7% fetal bovine serum (FBS) in an atmosphere of 5% CO_2 and 95% air at 37°C. Mat-LyLu cancer cells were cultured in RPMI 1640 medium containing 2 mmol·L^{-1} glutamine and 10% FBS. When cells became confluent, they were subcultured in the same medium. At confluence, the cells were passaged by using 0.05% trypsin in 0.02% EDTA. Medium was replaced twice weekly.

Solutions and drugs

The composition of the control extracellular Tyrode solution was as follows (in mmol·L^{-1}): NaCl 136.5, KCl 5.4, $CaCl_2$ 1.8, $MgCl_2$ 0.53, glucose 5.5 and HEPES-NaOH buffer 5.5 (pH 7.4). To block K^+ currents, the patch pipette contained (in mmol·L^{-1}): CsCl 140, EGTA 10, $MgCl_2$ 2, Na_2ATP 3, guanosine-5′-triphosphate (GTP, sodium salt, Sigma) 0.1 and HEPES-CsOH buffer 5 (pH 7.2). In addition, 4-aminopyridine (4-AP, 4 mmol·L^{-1}), tetraethylammonium (2 mmol·L^{-1}) and Ba^{2+} (1 mmol·L^{-1}) were added to the control solution to block K^+ current and record I_{Na}. Nifedipine, 4-AP, TEA, tetrodotoxin (TTX) and cis-5,8,11,14,17-eicosapentaenoic acid (EPA, Na salt) were obtained from Sigma Chemicals Co. EPA was dissolved in water just before use.

Recording technique and data analysis

Membrane currents were recorded with tight-seal whole-cell clamp techniques by using a patch-clamp amplifier (EPC-7, List Electronics, Darmstadt, Germany) (Hamill *et al.*, 1981; Nakajima *et al.*, 1999). The heat-polished patch electrode had tip resistance of 3–5 MΩ. All data were acquired, stored and analysed on Power Macintosh 7100/80 by using the PULSE + PULSEFIT software (HEKA Electronic) and Igor PRO (Wave Metrics, Lake Oswego, OR) as previously described (Terasawa *et al.*, 2002). All experiments were performed at room temperature (20–25°C). The steady-state inactivation of I_{Na} was estimated by using double-pulse protocols. Conditioning voltage pulses (500 ms in duration) of various membrane potentials between −80 and +20 mV were applied from a holding potential of −80 mV. At 2 ms after the end of each conditioning pulse, a test pulse of +0 mV (300 ms in duration) was applied to elicit I_{Na}. The ratio of I_{Na} amplitudes, with and without conditioning pulses, was plotted against each conditioning voltage.

Analysis of fatty acid composition

PC-3 cells were incubated for 2.7–72 h in medium containing 30 μmol·L^{-1} EPA, and the medium was changed every other day. The cells were harvested by trypsinization, centrifuged at 2000× *g* for 15 min at 4°C, and then washed twice and resuspended at a cell density of 2×10^7 cells·mL^{-1} in 20 mmol·L^{-1} phosphate buffer (pH 7.4) and then sonicated (10 watt for 2 min and then 40 watt for 30 s on ice). The lipids in the cell sonicate were analysed as described earlier (Asano *et al.*, 1998). Briefly, lipids were extracted with chloroform–methanol solution (2:1, v·v^{-1}) in the presence of butylated hydroxytoluene. Fatty acid composition of cell phospholipids was determined by gas chromatography after separation of

phospholipid fraction by using aminopropyl-bonded phase columns.

RNA extraction, RT-PCR and real-time quantitative RT-PCR

Total cellular RNA was extracted by using ISOGEN (Nippon Gene, Tokyo, Japan). For RT-PCR, complementary DNA (cDNA) was synthesized from 1 μg of total RNA with reverse transcriptase with random primers (Toyobo, Osaka, Japan) as previously described (Jo *et al.*, 2004). The reaction mixture was then subjected to PCR amplification with specific forward and reverse oligonucleotide primers for 35 cycles consisting of heat denaturation, annealing and extension. PCR products were size-fractionated on 2% agarose gels and visualized under UV light. Primers were chosen based on the sequence of human SCN1–6A and 8–9A and rat SCN1A–6A and 8–9A as shown in Table 1. Real-time quantitative RT-PCR was performed with the use of real-time Taq-Man technology and a sequence detector (ABI PRISM® 7000, Applied Biosystems, Foster City, CA, USA) (Jo *et al.*, 2004). Gene-specific primers and Taq-Man probes were used to analyse transcript abundance. The 18S ribosomal RNA level was analysed as an internal control and used to normalize the values for transcript abundance of SCN family genes (SCN1–6A, 8A, 9A).

Immunocytochemistry

Immunocytochemical analyses were performed on the cells by using anti-PanNa$_v$ (Alomone Labs, Jerusalem, Israel), a rabbit polyclonal antibody against a peptide conserved in all Na$_v$ isoforms, anti-Na$_v$1.6 and anti-Na$_v$1.7 (Alomone Labs, Jerusalem, Israel). The cells were cultured on Lab-Tek Chamber Slide Glass (Nalge Nunc International, Naperville, IL, USA), fixed with 2% paraformaldehyde in PBS for 30 min and then blocked for 10 min with 2% horse serum in PBS. The cells were incubated for 60 min with the primary antibodies diluted with 0.01% Triton X and 0.01% NaN_3 in PBS. For negative controls, cells were treated without antibody. Alexa-Fluor-488-conjugated labelled donkey anti-rabbit IgG antibody (Molecular Probes, A21206) was used to visualize the channel expression. The cells were also stained with Hoechst 33 258 (Sigma Aldrich) to visualize nuclei. A confocal laser scanning microscope (Olympus FluoView FV300, Olympus Co., Tokyo, Japan) was used for observations.

Transfection of synthetic small interfering RNA (siRNA)

SCN8A and SCN9A siRNA and non-silencing (negative control) siRNAs, as described in Table 1, were purchased from Qiagen (Cambridge, MA, USA). They were transfected into PC-3 cells to a final concentration of 5 nmol·L^{-1}, by using the HiPerFect Transfection Reagent (5 μL·mL^{-1} culture; Qiagen) according to the instructions of the manufacturer. Transfected cells were incubated for 48 h in an atmosphere of 5% CO_2 and 95% air at 37°C before each experiment. Then, analysis of mRNA by using real-time RT-PCR and the functions of the cells were performed. Rhodamine-conjugated siRNA was used to confirm the transfection of siRNA by using Nikon ECLISE TE200-u.

Proliferation assay

Cell proliferation was assessed by the Cell Titer 96 Aqueous kit (Promega, Madison, WI, USA). The prostate cancer cells were plated in 96-well plates (Becton Dickinson Labware, Franklin Lakes, NJ, USA) at a density of 1×10^4 cells per well. On the next day, experimental media with TTX, EPA or siRNA were added. The plates were then incubated for 24 or 48 h, after which the

Table 1 PCR primers used for amplification of voltage-gated Na$^+$ channel genes and synthetic small interfering RNA (siRNA) for SCN8A and 9A

Gene symbol (human/rat)	*Channel*	*Size (bp)*		*Sequence (5′-3′)*	
hSCN1A (rSCN1A)	Na$_v$1.1	298 (436)	sense	GAC AGC ATC AGG AGG AAA GG	(GCAAGCTGTCCGCTGGTAATATA)
			antisense	TGG TCT GAC TCA GGT TGC TG	(AGTGATCGTGATATCAACCTGAAG)
hSCN2A (rSCN2A)	Na$_v$1.2	194 (494)	sense	ATC CAG AGG GCT TAC AGA CG	(GCTGCAGCTCTCCATTCACACAC)
			antisense	ATC ATA CGA GGG TGG AGA CG	(GGCTAAACAATACTGCAGGGAAAA)
hSCN3A (rSCN3A)	Na$_v$1.3	354 (422)	sense	AAT TCT GTG GGG GCT CTA GG	(TATCCGTGTCAACTGGACTCTAAG)
			antisense	AGC AGC AAG GTT GTC TGA GC	(GATTACTGGAGAAACTTGTGGACT)
hSCN4A (rSCN4A)	Na$_v$1.4	502 (407)	sense	CAG GCA TCT TCA CAG CAG AG	(GCCTGCGCTCTCTGACTTG)
			antisense	ACC ATG AGG AAG ACG GTG AG	(CCTGACATTGGTACCCGG)
hSCN5A (rSCN5A)	Na$_v$1.5	618 (501)	sense	ACC ATC GTG AAC AAC AAG AGC C	(GCCTAGTCTGGAACTCCCTGGAC)
			antisense	GGC AGC CAG CTT GAC AAT ACA C	(ACATCTCCAGAGAGCTACGGGACAC)
hSCN6A (rSCN6A)	Na$_x$	449 (692)	sense	AAG AGG TGT CTG GGC AGG AT	(AAAGGACCAAAGGTGTTCCATGATCTGATG)
			antisense	GAC CAG CAT CTG TCC TGT TG	(CCGCTCATCCTTTCCCATCACTCTTTTCGT)
hSCN8A (rSCN8A)	Na$_v$1.6	599 (401)	sense	GAG GTG AAG CCT CTG GAT GA	(TTCAATGCGGTTTCCATCCT)
			antisense	CGG ATG GTC TTT CTC TGC TC	(GACTGCAGGCCATGGTTCA)
hSCN9A (rSCN9A)	Na$_v$1.7	403 (402)	sense	GAG GCC TGT TTC ACA GAT GG	(TCAGCGTGCTTACAGACGGTA)
			antisense	TGG GGC CAA GAT CTG AGT AG	(CTAATGGCTGTGCTGCCTTTG)

siRNA (human)	Sequence
SCN8A_2 (82)	AACAACCAACTAATTGACTAA
SCN8A_4 (84)	CCCAGTTCATTGAGTACTGTA
SCN8A_6 (86)	CAGAGGGATACCAGTGTATGA
SCN9A_1 (91)	TAGGCTAATGACCCAAGATTA
SCN9A_4 (94)	CGGCAGCGGCTGAATATACAA
control(non-silence)	AATTCTCCGAACGTGTCACGT

tetrazolium salt and dye solution was added and colour development was allowed to proceed for 1 h at 37°C, 5% CO_2. Each plate was then read at an absorbance of 490 nm.

Invasion assay

Matrigel invasion chambers were prepared according to the manufacturer's instructions (Becton Dickinson Labware, MA) by coating Matrigel on the 8 μm pore membrane of the culture inserts for 24-well plates (Falcon). A 0.5 mL aliquot of PC-3 cell suspension at 1×10^5 cells·mL^{-1} treated with or without siRNA for 48 h was seeded on the upper chamber and incubated at 37°C in a humidified chamber. Seven per cent FBS with or without TTX and EPA was added to the upper compartment. After migration for 24 h at 37°C, cells were removed from the upper compartment. The number of invasive PC-3 cells on the lower surface of the filter membrane was determined by Diff Quik staining (Siemens, IL) and counted at a magnification of ×100. The percentage invasion was calculated as the ratio of the number of invasive cells in the presence of TTX, EPA or siRNA, relative to that in the absence of the drug.

Endocytosis assay

PC-3 cells were placed in Eppendorf tubes at a density of 1×10^5 cells per tube in Tyrode solution and left to equilibrate for 10–15 min. The solution was then replaced by 100 μL of Tyrode solution containing 0.5 mg·mL^{-1} horseradish peroxidase (HRP) type IV (Sigma-Aldrich). The cells were incubated in an atmosphere of 5% CO_2 and 95% air at 37°C for 60 min with and without TTX, EPA or siRNA as previously described (Onganer and Djamgoz, 2005). A background, which indicates endogenous peroxidase activity, was measured with normal Tyrode solution. After the incubation, the cells were rinsed three times to remove all extracellular HRP. In order to release the HRP contents of the cells, 120 μL of lysis buffer (made by serially adding 0.9 g NaCl, 10 mL 10% NP-40 and 2.5 mL 10% Na-deoxycholate to a solution of 0.79 g Tris base in 75 mL distilled water and adding 1 mL of 100 mmol·L^{-1} EDTA and completing the volume to 100 mL with distilled water) was added to the cell pellet. Immediately afterwards, diaminobenzidine (0.5 mg·mL^{-1}) and hydrogen peroxide (0.01%) in 120 μL of 1 mol·L^{-1} Tris buffer (pH 7.4) were added, and the reaction solutions were transferred to a 96-well plate. The density of the colour reaction was measured at 570 nm on a plate reader (Bio-Rad Laboratories Inc, Helcules, CA, USA), and the absorbance was taken to represent the endocytotic activity.

Data analysis

All values are expressed as means ± SEM. Student's paired *t*-test was used to compare two sets of data from the same subjects. Comparison of time courses of parameters was analysed by one-way ANOVA for repeated measures. When differences were indicated, a Bonferroni's comparison was used to determine significance. Differences were considered significant if $P < 0.05$.

Results

EPA inhibits Na^+ current in prostate cancer cells

Figure 1A,B show I_{Na} in prostate cancer cells. The cells were held at –80mV, and the command voltage pulses (50 ms in duration) were applied to +0 mV. A fast transient inward current could be elicited in both human PC-3 cancer cells (Figure 1A) and Mat-LyLu rat cancer cells (Figure 1B). TTX (1 μmol·L^{-1}, Figure 1A,B) or replacement of extracellular Na^+ with N-methyl-D-glucamine (NMDG; Figure 1C), an impermeable cation, completely abolished I_{Na}, indicating that the transient inward current was carried by TTX-sensitive Na^+ channels (Na_v), as previously reported for these prostate cancer cell lines (Grimes *et al.*, 1995; Laniado *et al.*, 1997; Fraser *et al.*, 2003; Brackenbury and Djamgoz, 2006).

The typical current data recorded at each membrane potential and current–voltage (I–V) relations measured at the peak of the inward current are shown for Mat-LyLu cells (Figure 1D,E). At potentials more positive than –40 mV, I_{Na} was elicited (Figure 1A). The peak amplitude of the inward current was observed at approximately –10 mV. Figure 1F shows the steady-state inactivation curve for I_{Na}. The relation between membrane potentials and the h_∞ value (Figure 1F) was fitted to the following equation (Boltzmann equation) by using the least-squares methods: $I(V)/I_{max} = 1/[1 + \exp[(V - V_h)k^{-1}]]$, where V is the membrane potential in mV, V_h is the membrane potential at half maximum, and k is the slope factor. The value of V_h and k was –61 ± 6 mV and 7.9 ± 4 mV ($n = 4$) respectively.

The effects of TTX on I_{Na} in Mat-LyLu cells are shown in Figure 2A,B. The cells were held at –80 mV, and the command pulses to +0 mV (50 ms in duration) were applied at 0.1 Hz. Inhibition by TTX was concentration-dependent with an IC_{50} value of 7.0 nmol·L^{-1} ($n = 5$). Extracellular application of EPA (30 μmol·L^{-1}) also rapidly inhibited I_{Na}, and this inhibition attained a steady-state level within 2–3 min (Figure 2C). After washing with albumin (0.1%), I_{Na} gradually returned to the control level (Figure 2C). These effects of EPA were concentration-dependent (3–30 μmol·L^{-1}; Figure 2D) and yielded an IC_{50} of approximately 6 μmol·L^{-1} ($n = 5$, Figure 2E).

Expression of mRNA for voltage-gated Na channels in PC-3 cells

The results described above show that a TTX-sensitive Na_v is functional in prostate cancer cells. Therefore, we investigated the expression of mRNA for members of the SCN channel family (SCN1A–9A) in Mat-LyLu cells (Figure 3A) and PC-3 cells (Figure 4A). We did not assay for SCN7A, because SCN6A and 7A are probably encoded by the same gene or for SCN10A or 11A, as I_{Na} carried by these channels is TTX-insensitive (Catterall, 1992). The transcripts of SCN1A, 2A, 6A, 8A and 9A were detected in Mat-LyLu cells (Figure 3A). In PC-3 cells, transcripts of SCN8A and 9A were clearly detected (Figure 4A), and transcripts of SCN2A and 5A were only weakly expressed. The transcripts of SCN1A, 4A and 6A were not detected. The size of SCN cDNA fragments were as predicted, identical to cDNA fragments amplified from reversely transcribed mRNA.

Expression of SCN channel family members (SCN1A–9A) was also investigated by real-time quantitative RT-PCR in

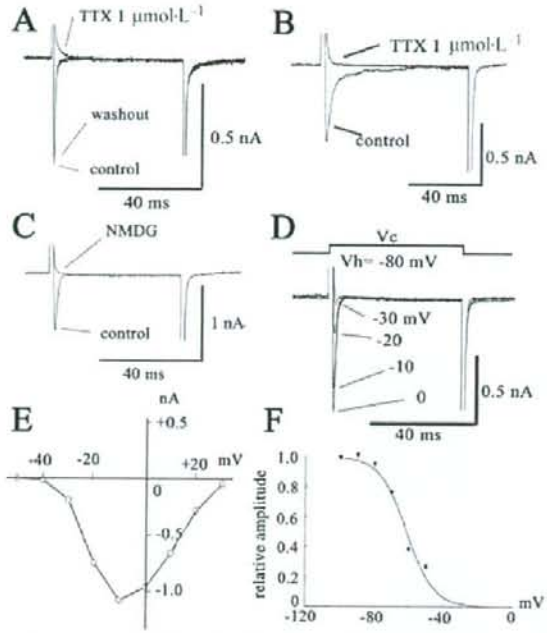

Figure 1 Characteristics of the Na current (I_{Na}) expressed in prostate cancer cells [human prostate cancer cell line (PC-3) and Mat-LyLu rat prostate cancer cell lines]. The cells were held at −80 mV, and command voltage pulses to +0 mV were applied in PC-3 (A) and Mat-LyLu cells (B and C). (C) Effects of replacement of extracellular Na^+ with $NMDG^+$. The current traces in B and C were elicited from a holding potential of −80 mV to +0 mV. In Mat-LyLu cells, the original current traces elicited by depolarizing pulses are indicated in D. The current–voltage (I–V) relations measured at the peak are illustrated in E. The I–V relations are shown after the leakage currents were subtracted. (F) Steady-state inactivation curves for I_{Na} expressed in Mat-LyLu cells. The data obtained from four cells were fitted by a Bolzmann equation. NMDG, N-methyl-D-glucamine; TTX, tetrodotoxin.

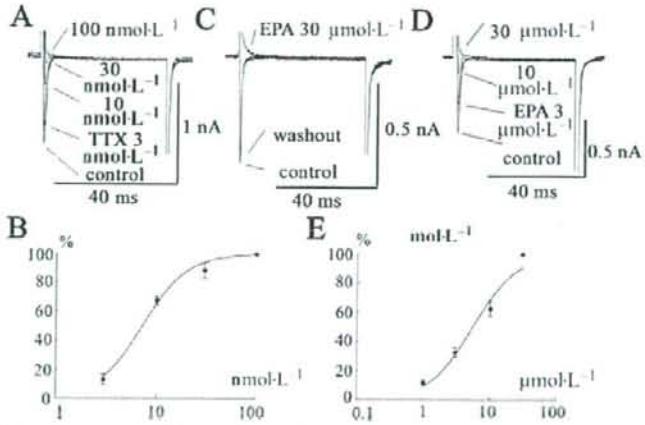

Figure 2 Effects of TTX and EPA on I_{Na} expressed in Mat-LyLu cells. (A) Concentration-dependent inhibition of I_{Na} by TTX. The cells were held at −80 mV, and command voltage-pulses to +0 mV (50 ms in duration) were applied at 0.2 Hz. (B) The inhibitory effect of TTX on the current amplitude measured at the peak is plotted against various concentrations of TTX. Data are shown as means ± SEM ($n = 5$) and fitted to a Michaelis-Menten simple bimolecular model: %inhibition = $100/\{1 + (IC_{50}\ [TTX]^{-1})\}$, where IC_{50} is 50% inhibitory concentration for TTX. The data yielded an IC_{50} value of 7.0 nmol·L^{-1}. (C) Effects of EPA on I_{Na}. The cell was held at −80 mV, and a depolarizing pulse to +0 mV was applied. After washing out with 0.1% albumin, the depressed I_{Na} returned to a control level. (D & E) Concentration-dependent inhibition of I_{Na} by EPA. The data represent a typical recording obtained from five different cells. The inhibitory effect of EPA on the current amplitude measured at the peak is plotted against various concentrations of EPA. Data are shown as means ± SEM ($n = 5$) and fitted using a Hill equation: % inhibition = $100/\{1 + (IC_{50}\ [EPA]^{-1})^n\}$, where n represents Hill coefficient, and IC_{50} is 50% inhibitory concentration for EPA. The data yielded an IC_{50} value of 6 μmol·L^{-1} and n of 1.1. EPA, eicosapentaenoic acid; I_{Na}, Na^+ current; TTX, tetrodotoxin.

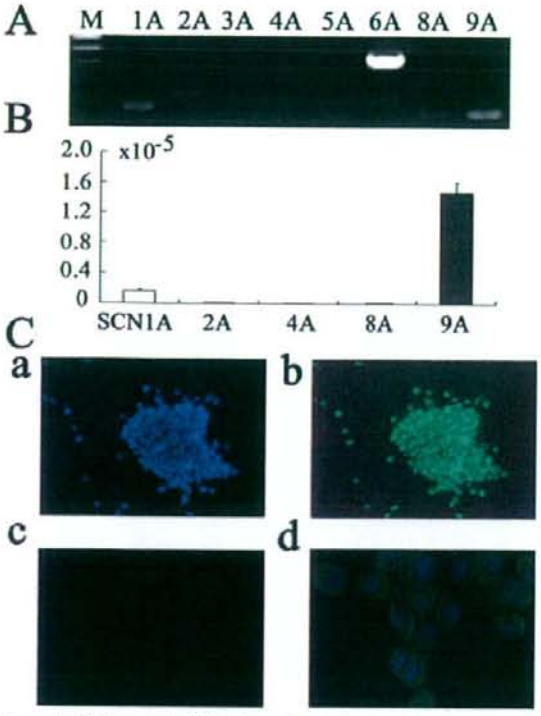

Figure 3 Voltage-gated Na^+ channel proteins in Mat-LyLu rat prostate cancer cell lines. (A) Expression of genes for voltage-gated Na^+ channels, detected by reverse transcriptase polymerase chain reaction (RT-PCR) in Mat-LyLu cells. M, Marker. (B) Summary results of real-time quantitative RT-PCR. The expression levels of SCN channel genes were normalized to those of the 18S ribosomal RNA levels. Data are means ± SEM from six independent samples. (C) Immunocytochemical detection with $PanNa_v$ in Mat-LyLu cells. Staining with Hoechst 33258 to visualize nuclei (Ca), $PanNa_v$ (Cb), negative control (without antibody, Cc), double staining with Hoechst 33258 and $PanNa_v$ (Cd).

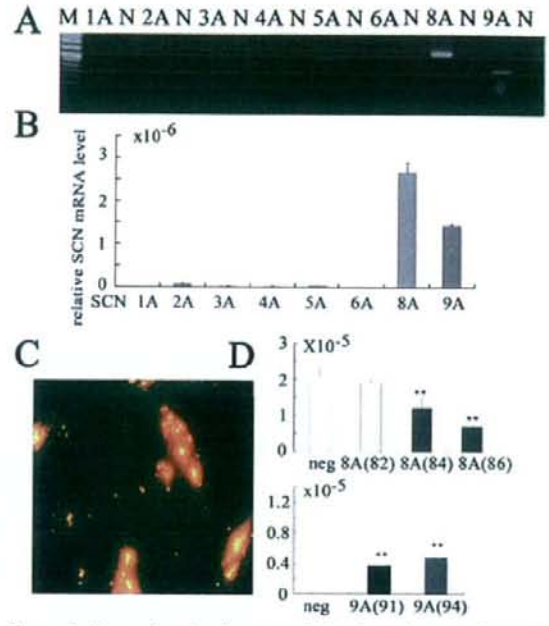

Figure 4 Expression of voltage-gated Na^+ channel genes detected by reverse transcriptase polymerase chain reaction (RT-PCR) in human prostate cancer cell line (PC-3). (A) Results of RT-PCR. M, Marker; N, negative control. (B) Real-time quantitative RT-PCR. The expression levels of SCN channel genes were normalized to those of the 18S ribosomal RNA levels. Summary data are means ± SEM from six independent samples. (C) Transfection of synthetic small interfering RNA (siRNA) for SCN8A mRNA. The transfected siRNA conjugated with rhodamine was visualized under fluorescent microscopy. (D) Expression level of SCN8A and SCN9A mRNA in PC-3 cells transfected with various kinds of siRNA by using real-time quantitative RT-PCR. The numbers in parentheses refer to the different sequences as shown in Table 1 (lower half). $^{**}P < 0.01$ vs. negative control.

Mat-LyLu cells (Figure 3B) and PC-3 cells (Figure 4B). Transcript levels were normalized to 18S ribosomal housekeeping gene. As SCN6A has not been shown to form a functional Na^+ channel (Ogata and Ohishi, 2002), SCN9A appeared to encode for the TTX-sensitive, Na_v in Mat-LyLu cells. On the other hand, in PC-3 cells, expression levels of SCN8A and SCN9A mRNA were much higher than those of SCN2A and 5A, suggesting that SCN8A and SCN9A encode for TTX-sensitive Na_v in PC-3 cells.

Immunocytochemical detection of $PanNa_v$

Expression of Na_v protein was confirmed by immunostaining cultured cells, by using anti-$PanNa_v$ in Mat-LyLu cells (Figure 3Cb), which was consistent with the patch-clamp experiments. No expression of $PanNa_v$ was detected in negative controls without the antibody (Figure 3Cc). The cells were also counterstained with Hoechst 33 258 to visualize nuclei (Figure 3Ca), and the double staining with this dye and $PanNa_v$ is shown in Figure 3Cd. Similarly, expression of Na_v proteins, by using anti-$Na_v1.6$ (Figure 5A), anti-$Na_v1.7$ (Figure 5B) and anti-$PanNa_v$ (Figure 5C) antibodies, was confirmed in PC cells. No expression of $PanNa_v$ was detected in negative controls without the antibody (Figure 5d). These results were consistent with the results of the RT-PCR studies.

Effect of siRNA for SCN8A and SCN9A on the expression of voltage-gated Na^+ channels

To inhibit the expression of SCN8A and SCN9A, we used siRNA methods. Transfection of siRNA conjugated with rhodamine was confirmed by fluorescent microscopy (Figure 4C). Two days after siRNA treatment, the inhibitory effect on the expression of SCN mRNA was analysed by real-time RT-PCR. The expression level of SCN8A and SCN9A mRNA in PC-3 cells was significantly inhibited by the corresponding siRNA, compared with non-silencing (negative control) siRNA, as shown in Figure 4D. The most effective inhibition of mRNA for SCN8A was with the SCN8A (86) structure (Figure 4D, $P < 0.001$, $n = 4$), and the most effective siRNA for SCN9A was SCN9A (91) (see Table 1 for structures; Figure 4D, $P < 0.001$, $n = 4$). As 48 h treatment was sufficient to reduce the expression level, we used the cells 48 h after the

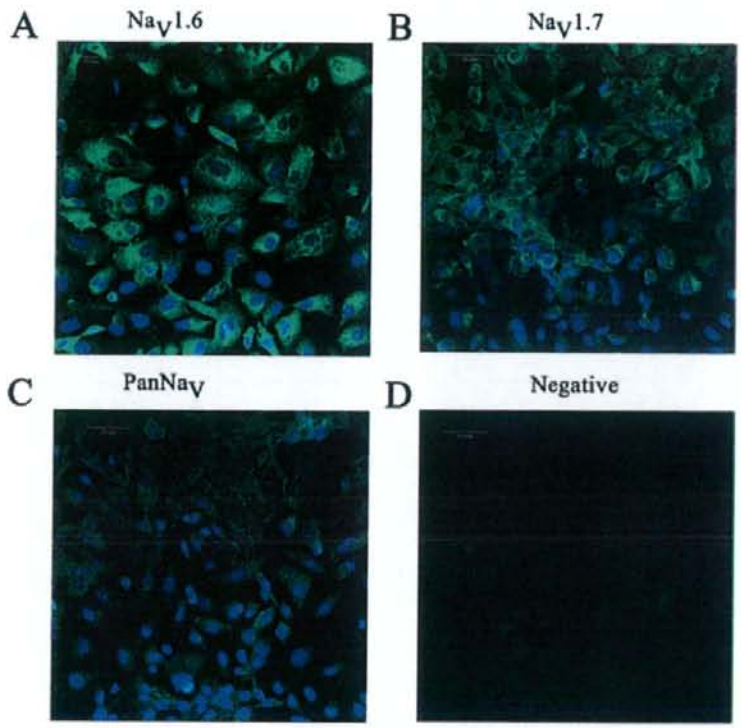

Figure 5 Immunocytochemical detection of $Na_V1.6$, $Na_V1.7$ and $PanNa_V$ in PC-3 cells. In A, double staining with Hoechst 33 258 and antibody to $Na_V1.6$. In B, staining with $Na_V1.7$ and in C with $PanNa_V$ antibodies is shown. Negative control (without antibody, D).

transfection to investigate the effect of siRNA for SCN8A (86) and SCN9A (91) in the subsequent experiments.

Effects of long-term treatment with EPA on fatty acid compositions of PC cells and mRNA levels of the Na^+ channel

Figure 6A shows the changes in fatty acid composition of phospholipids after treatment with EPA [C20:5 (ω-3)] for 2.7–72 h. The EPA, docosapentaenoic acid [DPA, C22:5 (ω-3)] and docosahexaenoic acid [DHA, C22:6 (ω-3)] content of the phospholipids increased in a time-dependent manner. On the other hand, arachidonic acid [AA, C20:4 (ω-6)] decreased time-dependently. Thus, the ratio of EPA to AA increased from 0.1 to 1.3 (24 h) and then 3.2 (72 h). The ratio of ω-3 to ω-6 also increased significantly.

Figure 6B shows the effects of 48 h treatment with EPA on the expression of SCN8A and 9A mRNA by real-time quantitative RT-PCR in PC-3 cells. The transcript levels were normalized to 18S ribosomal housekeeping gene. EPA (30 (M) was added to the cells before they reached confluence in culture medium supplemented with 7% FBS for 48 h. Treatment with EPA for 48 h significantly inhibited the expression of both SCN8A and SCN9A mRNA. Thus, these results suggested that longer exposures (48–72 h) to EPA decreased the level of the mRNA for Na channels carrying I_{Na}, after the EPA was incorporated into the cell lipids.

Effects of EPA on cell migration and proliferation

In order to determine the roles of Na^+ channels on cell migration and proliferation, PC-3 cells were treated with either TTX or siRNA. The cells transfected with siRNA for SCN9A (91) and/or SCN8A (86) were compared with the cells transfected with non-silencing (negative control) siRNA. TTX (10 μmol·L^{-1}, Figure 7A) significantly inhibited cell migration ($n = 6$, $P < 0.05$). In addition, siRNA for SCN9A inhibited cell migration ($n = 6$, $P < 0.05$), but a combination of siRNA for SCN8A and for SCN9A provided greater inhibition (Figure 7B). As shown in Figure 7C,D, EPA (30 μmol·L^{-1}) also significantly inhibited cell migration ($n = 6$, $P < 0.05$) in a similar way to TTX (10 μmol·L^{-1}).

Effects of TTX and the combination of siRNA targeted for SCN8A and SCN9A, on cell proliferation were investigated in PC-3 cells. Neither TTX (10 μmol·L^{-1}) nor siRNA had effect on cell proliferation at 24 and 48 h (Figure 8A,B, $n = 6$). However, EPA (30 μmol·L^{-1}) markedly inhibited cell proliferation, in contrast to TTX (Figure 8C).

Effects of EPA on endocytosis in PC-3 cells

Effects of TTX and siRNA targeted for both SCN8A and SCN9A on cell endocytosis were examined in PC-3 cells, by using HRP uptake. As shown in Figure 9A,B, TTX (1–10 μmol·L^{-1}, $n = 7$, Figure 9A) and the siRNA (Figure 9B) significantly

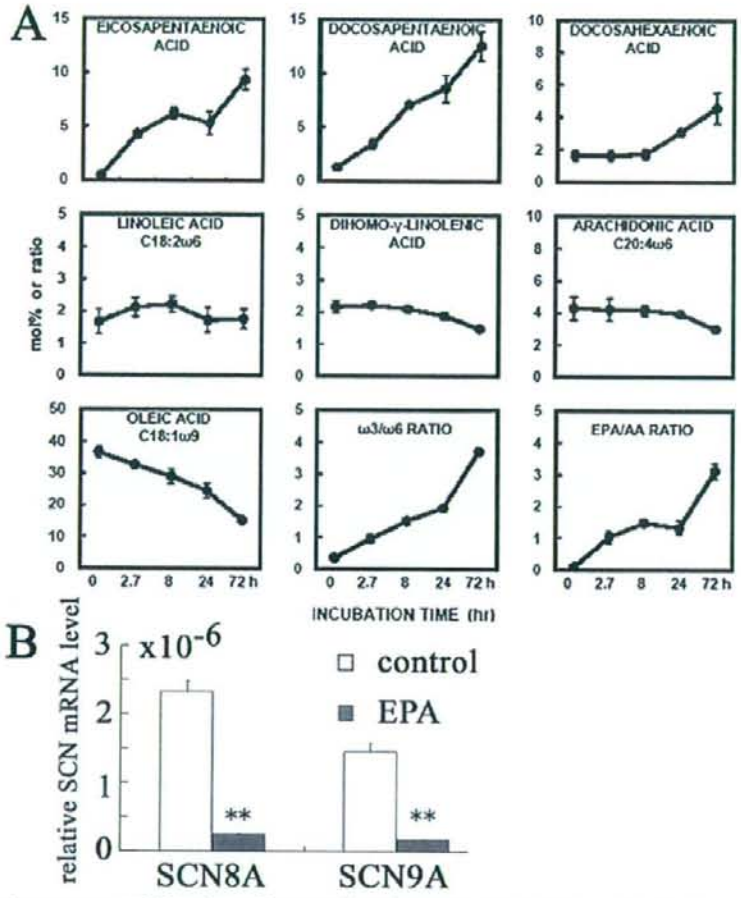

Figure 6 Effects of long-term exposure to EPA on fatty acid compositions of PC-3 cells and mRNA levels of the Na^+ channel proteins, in PC-3 cells. (A) Changes in fatty acid compositions of phospholipids in control cells and cells treated with EPA. The cells were treated with EPA (30 $\mu mol \cdot L^{-1}$) for 2.7–72 h. The changes of fatty acid composition in phospholipids (mol%) are indicated. The data represent means ± SEM value obtained from two different cells. (B) Effects of chronic treatment with EPA on the expression of SCN8A and 9A mRNA in PC-3 cells. SCN9A expression was assessed by real-time quantitative RT-PCR, and transcript levels were normalized to 18S ribosomal housekeeping gene. EPA (30 $\mu mol \cdot L^{-1}$) was added to the cells before they reached confluence in culture medium for 48 h. After incubation for 48 h in culture medium supplemented with 7% FBS, expression of mRNA for SCN8A and SCN9A in the presence of EPA was compared with that in the absence of EPA. $^{**}P < 0.01$ vs. control. EPA, eicosapentaenoic acid; FBS, fetal bovine serum; RT-PCR, reverse transcriptase polymerase chain reaction.

reduced HRP uptake into PC-3 cells ($P < 0.01$, $n = 7$), suggesting that I_{Na} is necessary for endocytosis in PC-3 cells. Also, EPA significantly inhibited HRP uptake into the cells in a concentration-dependent manner ($n = 7$; Figure 9C).

Discussion

The major findings of the present study were twofold. Firstly, EPA inhibited voltage-gated Na^+ current (I_{Na}) in prostate cancer cells via two independent mechanisms: by directly affecting the channel and rapidly inhibiting I_{Na} with an IC_{50} of approximately 6 $\mu mol \cdot L^{-1}$ or indirectly by decreasing the level of the mRNAs for channel proteins (SCA8A and SCN9A), carrying I_{Na}, after incorporation of EPA into cell lipids. Secondly, EPA, TTX and siRNA targeted for Na channel α-subunits inhibited metastatic functions (invasion and endocytosis) of the two cell lines. These results suggest that EPA could inhibit metastatic activity by blocking the up-regulated I_{Na} in prostate cancer cells. Such blockade may reduce the risk of prostate carcinoma and its progression, and consequently increase survival.

The present study shows the presence of I_{Na} in prostate cancer cells (Mat-LyLu rat prostate cancer cell lines and PC-3 human prostate cancer cell lines), which was consistent with previous papers (Grimes *et al.*, 1995; Fraser *et al.*, 2000; 2003; Anderson *et al.*, 2003; Bennett *et al.*, 2004; Krasowska *et al.*, 2004; Brackenbury and Djamgoz, 2006). TTX completely inhibited I_{Na} expressed in both cancer cell lines and, in Mat-LyLu cells, TTX had an IC_{50} value of approximately

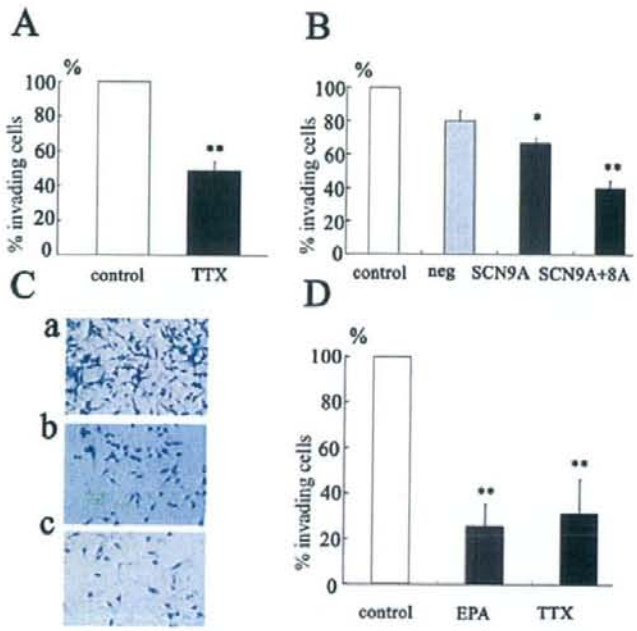

Figure 7 Effects of treatment with TTX, siRNA targeted for SCN8A or SCN9A and EPA on cell invasion in PC-3 cells. (A) Effects of TTX (10 μmol·L^{-1}) on cell invasion. (B) Effects of siRNA for SCN9A alone and in combination with siRNA for SCN8A on cell invasion. (C & D) Effects of EPA and TTX on invasion assay. In C, photographs showing typical fields of view of PC-3 cells following invasion through the Matrigel-coated chamber under control conditions (a), and in the presence of TTX (10 μmol·L^{-1}, b), and EPA (30 μmol·L^{-1}, c). In D, summary data from these assays (means ± SEM from six different experiments). *$P < 0.05$, **$P < 0.01$ vs. control. EPA, eicosapentaenoic acid; siRNA, synthetic small interfering RNA; TTX, tetrodotoxin.

7 nmol·L^{-1}. These findings indicate that I_{Na} expressed in these prostate cancer cells closely resembles TTX-sensitive I_{Na} found in human brain and skeletal muscle, but is different from the TTX-insensitive I_{Na} found in heart. By using molecular techniques, it appears that human breast cancer cells express a TTX-insensitive Na^+ channel subunit, SCN5A, while prostate cancer cells express a TTX-sensitive protein, SCN9A (Diss *et al.*, 2001; 2005). In primary cultures of human cervical cancer, TTX-sensitive I_{Na} has been reported to be carried by a number of channels, $Na_V1.2$, $Na_V1.4$, $Na_V1.6$ and $Na_V1.7$ (Diaz *et al.*, 2007). In the present studies, the transcript of $Na_V1.1$, $Na_V1.2$, $Na_V1.6$ and $Na_V1.7$ was detected in Mat-LyLu cells, as previously reported (Diss *et al.*, 2001; 2005). However, in PC-3 cells, the predominant expression was of $Na_V1.6$ and $Na_V1.7$, and there was more of SCN8A, compared with SCN9A. The presence of these Na channels was confirmed by immunohistochemical studies in these prostate cancer cells. Thus, the expression of SCN8A and SCN9A genes appears to yield TTX-sensitive I_{Na} in PC-3 cells.

The present study showed for the first time that EPA inhibited I_{Na} in prostate cancer cells. The inhibitory effect of EPA was observed at concentrations greater than 0.1 μmol·L^{-1}, and the IC_{50} of EPA was approximately 6 μmol·L^{-1}. As the plasma concentration of free EPA measured by gas chromatography was about 1–6 μmol·L^{-1} and can be increased after ingestion of cod liver oil or after treatment with EPA-ester (Okuda *et al.*, 1997), the inhibitory action of EPA on I_{Na} may play a crucial role in clinical settings. Several possible mechanisms to explain the effects of EPA on I_{Na} can be proposed. But, as shown previously (Jo *et al.*, 2005), neither indomethacin, a cyclo-oxygenase inhibitor, nor NDGA, a lipoxygenase inhibitor, prevented the effects of EPA on I_{Na} (data not shown) suggesting that the metabolites of these pathways are not involved in this action of EPA. Alternatively, EPA has been reported to inhibit $I_{Ca,L}$ in smooth muscle cells and cardiac myocytes (Xiao *et al.*, 1997). Thus, it is more likely that EPA modulates I_{Na} by an interaction with the channel protein itself or by acting at lipid sites near the channels, after partition into the lipid bilayer. The binding sites of EPA have been proposed to be on the short cytoplasmic segment of the α-subunit of Na channels, linking transmembrane repeats III and IV in cardiac myocytes (Kang and Leaf, 1996). The IC_{50} value of EPA on cardiac cells is approximately 4 μmol·L^{-1}, which is close to that in the present study using prostate cancer cells. We also reported that I_{Na} expressed in cultured human bronchial smooth muscle cells is carried by $Na_V1.7$ coded by SCN9A mRNA and inhibited by EPA (Jo *et al.*, 2004; 2005). Thus, whether EPA inhibits I_{Na} in prostate cancer cells by binding the sites similar to those in $Na_V1.5$ (Kang and Leaf, 1996) remains unclear, but I_{Na} appears to be an important target for EPA in prostate cancer cells.

Besides the acute effect of EPA, this fatty acid is incorporated into membrane phospholipids and consequently affects various membrane functions and gene expression (Asano *et al.*, 1998). Examples of this latter effect include prevention of the up-regulation of mRNA induced by mexiletine, an

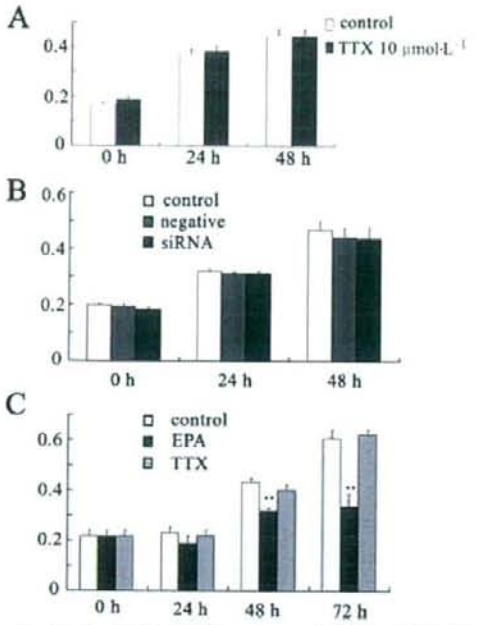

Figure 8 Effects of TTX, siRNA targeted for SCN8A and SCN9A and EPA on cell proliferation in PC-3 cells. (A) Effects of TTX on cell proliferation, assessed after cells were treated with TTX (10 μmol·L^{-1}) for 0, 24 and 48 h. (B) Effect of combined SCN8A and SCN9A siRNA on cell proliferation. Cells were transfected with siRNA targeted for both SCN8A (86) and SCN9A (91), or with non-silencing (negative control) siRNA. (C) Effects of EPA on cell proliferation after exposure to EPA (30 μmol·L^{-1}) for up to 72 h. **$P < 0.01$ vs. 0 h EPA, eicosapentaenoic acid; siRNA, synthetic small interfering RNA; TTX, tetrodotoxin.

anti-arrythmic agent (Kang *et al.*, 1997) in ventricular cells with EPA (20 μmol·L^{-1}) for 4 days although the basal level of mRNA for SCN5A was not altered. More recently, EPA inhibited SCN9A expression in cultured human bronchial smooth muscle cells (Jo *et al.*, 2005) and a ω-3 PUFA, DHA, inhibited SCN5A mRNA expression and I_{Na} in human breast cancer cells, where $Na_V1.5$ was predominant (Isbilen *et al.*, 2006). In our study, after chronic treatment with EPA, the EPA content of the phospholipid fraction (mol%) increased time-dependently, and that of AA decreased, increasing the ratio of EPA to AA. In our present work, EPA significantly decreased the level of both SCN8A and SCN9A mRNA in PC-3 prostate cancer cells, suggesting that EPA regulates the transcription of mRNA or its processing and stability of mRNA. Thus, it is likely that EPA may suppress the up-regulation of I_{Na} genes, by inhibiting transcription of the relevant genes in prostate cancer cells.

Na^+ current is up-regulated in several types of cancer cells, including prostate cancer, and is known to enhance other cellular functions linked to invasion, secretion, adhesion and motility (Grimes *et al.*, 1995; Laniado *et al.*, 1997; Smith *et al.*, 1998; Abdul and Hoosein, 2001; Anderson *et al.*, 2003; Fraser *et al.*, 2003; Mycielska *et al.*, 2003; Bennett *et al.*, 2004; Onganer and Djamgoz, 2005; Slade *et al.*, 2005; Fulgenzi *et al.*, 2006). The present study showed that I_{Na} was involved in cell invasion and endocytosis but not proliferation, in PC-3 cells. TTX and siRNA targeted for SCN9A or SCN8A significantly inhibited cell invasion. Interestingly, inhibition by a combination of siRNA for SCN9A and for SCN8A, was greater than that after either siRNA alone, suggesting that both subunits were contributing the I_{Na} observed. Similarly, endocytosis measured by uptake of HRP was significantly inhibited by TTX or siRNA for Na_v proteins. In the present study, we also showed that EPA significantly inhibited cell invasion and endocytosis, through a 'chronic' effect on gene expression, as

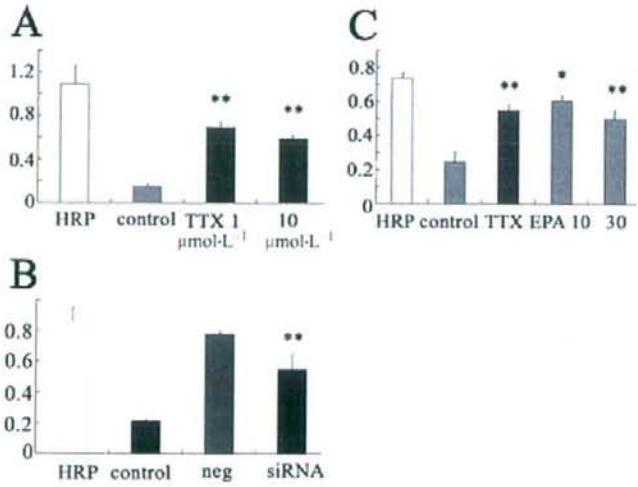

Figure 9 Effects of treatment with TTX (A), siRNA for SCN8A and SCN9A (B) and EPA (C) on endocytosis of HRP in PC-3 cells. Background (control) indicates endogenous peroxidase activity. *$P < 0.05$, **$P < 0.01$. EPA, eicosapentaenoic acid; HRP, horseradish peroxidase; siRNA, synthetic small interfering RNA; TTX, tetrodotoxin.

well as by a direct inhibition of the Na channel. The precise mechanism through which I_{Na} could regulate cellular functions is not known yet, but several possibilities can be considered. Particularly, Na^+ influx through I_{Na} may regulate cell volume (Bortner and Cidlowski, 2003), and changes in ion flux and cell volume may be integral to the invasion process (Soroceanu *et al.*, 1999). In turn, the subcellular/molecular mechanisms underlying these effects may involve the cytoskeleton (directly via β-subunit interaction and/or indirectly via local Ca^{2+} fluxes), protein kinase activity and gene expression (Fraser *et al.*, 2003; Mycielska and Djamgoz, 2004). In contrast to the effects of TTX and siRNA on cell invasion and endocytosis, cell proliferation of prostate cancer cells was not affected by TTX and siRNA, suggesting that the contribution of I_{Na} to proliferation of cancer cells was minimal, a result compatible with previous work (Fraser *et al.*, 1999; Fulgenzi *et al.*, 2006). Nevertheless, EPA did significantly suppress cell proliferation, as well as invasion and endocytosis. Thus, EPA appears to inhibit cell growth, independent of I_{Na} blockade, possibly by modulating AA metabolism and/or *Pertussis* toxin-sensitive signal transduction pathways (Sauer *et al.*, 2005). Thus, it is likely that the suppressive effects of EPA on several functions that are crucial to metastasis, such as proliferation, motility, secretion and invasion may be involved in the inhibitory effects of EPA on the metastatic activities of prostate cancer cells.

In conclusion, the present study suggests that treatment with EPA induces direct acute inhibition of I_{Na} and long-term down-regulation of expression of Na channel proteins, up-regulated in prostate cancer cells, thus inhibiting their metastatic activities. I_{Na} would appear to be one of the targets of EPA for long-term control and suppression of prostate cancer cells.

Acknowledgements

This study was supported by The Vehicle Racing Commemorative Foundation, and grants-in-aid from the Ministry of Education, Science and Culture, the Ministry of Health and Welfare of Japan to T Nakajima.

Conflict of interests

None.

References

Abdul M, Hoosein N (2001). Inhibition by anticonvulsants of prostate-specific antigen and interleukin-6 secretion by human prostate cancer cells. *Anticancer Res* **21**: 2045–2048.

Alexander SPH, Mathie A, Peters JA (2008). Guide to Receptors and Channels (GRAC), 3rd edn. *Br J Pharmacol* **153** (Suppl. 2): S1–S209.

Anderson JD, Hansen TP, Lenkowski PW, Walls AM, Choudhury IM, Schenck HA *et al.* (2003). Voltage-gated sodium channel blockers as cytostatic inhibitors of the androgen-independent prostate cancer cell line PC-3. *Mol Cancer Ther* **2**: 1149–1154.

Armstrong B, Doll R (1975). Environmental factors and cancer incidence and mortality in different countries, with special reference to dietary practices. *Int J Cancer* **15**: 617–631.

Asano M, Nakajima T, Hazama H, Iwasawa K, Tomaru T, Omata M *et al.* (1998). Influence of cellular incorporation of n-3 eicosapentaenoic acid on intracellular Ca^{2+} concentration and membrane potential in vascular smooth muscle cells. *Atherosclerosis* **138**: 2722–2728.

Bennett ES, Smith BA, Harper JM (2004). Voltage-gated Na^+ channels confer invasive properties on human prostate cancer cells. *Pflugers Arch* **447**: 908–914.

Bortner CD, Cidlowski JA (2003). Uncoupling cell shrinkage from apoptosis reveals that Na^+ influx is required for volume loss during programmed cell death. *J Biol Chem* **278**: 39176–39184.

Brackenbury WJ, Djamgoz MB (2006). Activity-dependent regulation of voltage-gated Na^+ channel expression in Mat-LyLu rat prostate cancer cell line. *J Physiol* **573**: 343–356.

Breslow N, Chan CW, Dhom G, Drury RA, Franks LM, Gellei B *et al.* (1977). Latent carcinoma of prostate at autopsy in seven areas. The International Agency for Research on Cancer, Lyons, France. *Int J Cancer* **20**: 680–688.

Catterall WA (1992). Cellular and molecular biology of voltage-gated sodium channels. *Physiol Rev* **72**: S15–S48.

Chavarro JE, Stampfer MJ, Li H, Campos H, Kurth T, Ma J (2007). A prospective study of polyunsaturated fatty acid levels in blood and prostate cancer risk. *Cancer Epidemiol Biomarkers Prev* **16**: 1364–1370.

Diaz D, Delgadillo DM, Hernández-Gallegos E, Ramírez-Domínguez ME, Hinojosa LM, Ortiz CS *et al.* (2007). Functional expression of voltage-gated sodium channels in primary cultures of human cervical cancer. *J Cell Physiol* **210**: 469–478.

Diss JK, Archer SN, Hirano J, Fraser SP, Djamgoz MB (2001). Expression profiles of voltage-gated Na^+ channel alpha-subunit genes in rat and human prostate cancer cell lines. *Prostate* **48**: 165–178.

Diss JK, Stewart D, Pani F, Foster CS, Walker MM, Patel A *et al.* (2005). A potential novel marker for human prostate cancer: voltage-gated sodium channel expression in vivo. *Prostate Cancer Prostatic Dis* **8**: 266–273.

Dunn JE (1975). Cancer epidemiology in populations of the United States – with emphasis on Hawaii and California – and Japan. *Cancer Res* **35**: 3240–3245.

Fraser SP, Ding Y, Liu A, Foster CS, Djamgoz MB (1999). Tetrodotoxin suppresses morphological enhancement of the metastatic MAT-LyLu rat prostate cancer cell line. *Cell Tissue Res* **295**: 505–512.

Fraser SP, Grimes JA, Djamgoz MB (2000). Effects of voltage-gated ion channel modulators on rat prostatic cancer cell proliferation: comparison of strongly and weakly metastatic cell lines. *Prostate* **44**: 61–76.

Fraser SP, Salvador V, Manning EA, Mizal J, Altun S, Raza M *et al.* (2003). Contribution of functional voltage-gated Na^+ channel expression to cell behaviors involved in the metastatic cascade in rat prostate cancer: I. Lateral motility. *J Cell Physiol* **195**: 479–487.

Fulgenzi G, Graciotti L, Faronato M, Soldovieri MV, Miceli F, Amoroso S *et al.* (2006). Human neoplastic mesothelial cells express voltage-gated sodium channels involved in cell motility. *Int J Biochem Cell Biol* **38**: 1146–1159.

Goldin AL (1999). Diversity of mammalian voltage-gated sodium channels. *Ann NY Acad Sci* **868**: 38–58.

Goldin AL (2002). Evolution of voltage-gated Na^+ channels. *J Exp Biol* **205**: 575–584.

Grimes JA, Fraser SP, Stephens GJ, Downing JE, Laniado ME, Foster CS *et al.* (1995). Differential expression of voltage-activated Na^+ currents in two prostatic tumor cell lines: contribution to invasiveness in vitro. *FEBS Lett* **369**: 290–294.

Haenszel W, Kurihara M. (1968). Studies of Japanese migrants. I. Mortality from cancer and other diseases among Japanese in the United States. *J Natl Cancer Inst* **40**: 43–68.

Hamill P, Marty A, Neher E, Sakmann B, Sigworth FJ (1981). Improved patch-clamp techniques for high-resolution current recording

from cells and cell-free membrane patches. *Pflugers Arch* **391**: 85–100.

Isbilen B, Fraser SP, Djamgoz MB (2006). Docosahexaenoic acid (omega-3) blocks voltage-gated sodium channel activity and migration of MDA-MB-231 human breast cancer cells. *Int J Biochem Cell Biol* **38**: 2173–2182.

Jo T, Nagata T, Iida H, Imuta H, Iwasawa K, Ma J *et al.* (2004). Voltage-gated sodium channel expressed in cultured human smooth muscle cells: Involvement of SCN9A. *FEBS Lett* **567**: 339–343.

Jo T, Iida H, Kishida S, Imuta H, Oonuma H, Nagata T *et al.* (2005). Acute and chronic effects of eicosapentaenoic acid on voltage-gated sodium channel expressed in cultured human bronchial smooth muscle cells. *Biochem Biophys Res Commun* **331**: 1452–1459.

Kang JX, Leaf A (1996). Evidence that free polyunsaturated fatty acids modify Na^+ channels by directly binding to the channel proteins. *Proc Natl Acad Sci USA* **93**: 3542–3546.

Kang JX, Li Y, Leaf A (1997). Regulation of sodium channel gene expression by class I antiarrhythmic drugs and n-3 polyunsaturated fatty acids in cultured neonatal rat cardiac myocytes. *Proc Natl Acad Sci USA* **94**: 2724–2728.

Kelavkar UP, Hutzley J, Dhir R, Kim P, Allen KG, McHugh K (2006). Prostate tumor growth and recurrence can be modulated by the omega-6:omega-3 ratio in diet: Athymic mouse xenograft model simulating radical prostatectomy. *Neoplasia* **8**: 112–124.

Krasowska M, Grzywna ZJ, Mycielska ME, Djamgoz MB (2004). Patterning of endocytic vesicles and its control by voltage-gated Na^+ channel activity in rat prostate cancer cells: fractal analyses. *Eur Biophys J* **33**: 535–542.

Laniado ME, Lalani EN, Fraser SP, Grimes JA, Bhangal G, Djamgoz MB *et al.* (1997). Expression and functional analysis of voltage-activated Na+ channels in human prostate cancer cell lines and their contribution to invasion in vitro. *Am J Pathol* **150**: 1213–1221.

Larsson SC, Kumlin M, Ingelman-Sundberg M, Wolk A (2004). Dietary long-chain n-3 fatty acids for the prevention of cancer: a review of potential mechanisms. *Am J Clin Nutr* **79**: 935–945.

Leitzmann MF, Stampfer MJ, Michaud DS, Augustsson K, Colditz GC, Willett WC *et al.* (2004). Dietary intake of n-3 and n-6 fatty acids and the risk of prostate cancer. *Am J Clin Nutr* **80**: 204–216.

Mycielska ME, Djamgoz MB (2004). Cellular mechanisms of direct-current electric field effects: galvanotaxis and metastatic disease. *J Cell Sci* **117**: 1631–1639.

Mycielska ME, Fraser SP, Szatkowski M, Djamgoz MB (2003). Contribution of functional voltage-gated Na^+ channel expression to cell behaviors involved in the metastatic cascade in rat prostate cancer: II. Secretory membrane activity. *J Cell Physiol* **195**: 461–469.

Nakajima T, Iwasawa K, Oonuma H, Imuta H, Hazama H, Asano M *et al.* (1999). Troglitazone inhibits voltage-dependent calcium currents in guinea pig cardiac myocytes. *Circulation* **99**: 2942–2950.

Ogata N, Ohishi Y (2002). Molecular diversity and function of the voltage-gated Na^+ channels. *Jpn J Pharmacol* **88**: 365–377.

Okuda Y, Kawashima K, Sawada T, Tsurumaru K, Asano M, Suzuki S *et al.* (1997). Eicosapentaenoic acid enhances nitric oxide production by cultured human endothelial cells. *Biochem Biophys Res Commun* **232**: 487–491.

Onganer PU, Djamgoz MB (2005). Small-cell lung cancer (human): potentiation of endocytic membrane activity by voltage-gated Na^+ channel expression in vitro. *J Membr Biol* **204**: 67–75.

Parkin DM, Bray F, Ferlay J, Pisani P (2005). Global cancer statistics, 2002. *CA Cancer J Clin* **55**: 74–108.

Rose DP (1997). Effects of dietary fatty acids on breast and prostate cancers: evidence from in vitro experiments and animal studies. *Am J Clin Nutr* **66**: 1513S–1522S.

Sauer LA, Dauchy RT, Blask DE, Krause JA, Davidson LK, Dauchy EM (2005). Eicosapentaenoic acid suppresses cell proliferation in MCF-7 human breast cancer xenografts in nude rats via a pertussis toxin-sensitive signal transduction pathway. *J Nutr* **135**: 2124–2129.

Shennan DH, Bishop OS (1974). Diet and mortality from malignant disease in 32 countries. *West Indian Med J* **23**: 44–53.

Slade MJ, Tolhurst R, Palmieri C, Jiang J, Latchman DS, Coombes RC *et al.* (2005). Voltage-gated sodium channel expression and potentiation of human breast cancer metastasis. *Clin Cancer Res* **11**: 5381–5389.

Smith P, Rhodes NP, Shortland AP, Fraser SP, Djamgoz MB, Ke Y *et al.* (1998). Sodium channel protein expression enhances the invasiveness of rat and human prostate cancer cells. *FEBS Lett* **423**: 19–24.

Soroceanu L, Manning TJ, Jr, Sontheimer H (1999). Modulation of glioma cell migration and invasion using Cl^- and K^+ ion channel blockers. *J Neurosci* **19**: 5942–5954.

Terasawa K, Nakajima T, Iida H, Iwasawa K, Oonuma H, Jo T *et al.* (2002). Nonselective cation currents regulate membrane potential of rabbit coronary arterial cell: modulation by lysophosphatidylcholine. *Circulation* **106**: 3111–3119.

Xiao YF, Kang JX, Morgan JP, Leaf A (1995). Blocking effects of polyunsaturated fatty acids on Na^+ channels of neonatal rat ventricular myocytes. *Proc Natl Acad Sci USA* **92**: 11000–11004.

Xiao YF, Gomez AM, Morgan JP, Lederer WJ, Leaf A (1997). Suppression of voltage-gated L-type Ca^{2+} currents by polyunsaturated fatty acids in adult and neonatal rat ventricular myocytes. *Proc Natl Acad Sci USA* **94**: 4182–4187.

Xiao YF, Wright SN, Wang GK, Morgan JP, Leaf A (1998). Fatty acids suppress voltage-gated Na^+ currents in HEK293t cells transfected with the alpha-subunit of the human cardiac Na^+ channel. *Proc Natl Acad Sci USA* **95**: 2680–2685.

Xiao YF, Ke Q, Wang SY, Auktor K, Yang Y, Wang GK *et al.* (2001). Single point mutations affect fatty acid block of human myocardial sodium channel alpha subunit Na^+ channels. *Proc Natl Acad Sci USA* **98**: 3606–3611.

Pulmonary Pharmacology & Therapeutics xxx (2009) 1–7

Contents lists available at ScienceDirect

Pulmonary Pharmacology & Therapeutics

journal homepage: www.elsevier.com/locate/ypupt

Hyperoxia exaggerates bacterial dissemination and lethality in *Pseudomonas aeruginosa* pneumonia

Yoshiaki Kikuchi [a,b], Kazuhiro Tateda [a,*], Etsu T. Fuse [a], Tetsuya Matsumoto [c], Naomasa Gotoh [d], Jun Fukushima [e], Hajime Takizawa [f], Takahide Nagase [b], Theodore J. Standiford [g], Keizo Yamaguchi [a]

[a] Department of Microbiology and Infectious Diseases, Toho University School of Medicine, 5-21-16 Ohmorinishi, Ohtaku, Tokyo 143-8540, Japan
[b] Department of Respiratory Medicine, Tokyo University School of Medicine, Tokyo, Japan
[c] Department of Microbiology, Tokyo Medical University, Tokyo, Japan
[d] Department of Microbiology and Infection Control Science, Kyoto Pharmaceutical University, Kyoto, Japan
[e] Department of Biotechnology, Faculty of Bioresource Sciences, Akita Prefectural University, Akita, Japan
[f] Department of Respiratory Medicine, University of Teikyo Medical School, Tokyo, Japan
[g] Pulmonary and Critical Care Medicine, University of Michigan Medical School, Ann Arbor, MI 48109-0360, USA

ARTICLE INFO

Article history:
Received 4 September 2008
Received in revised form
23 December 2008
Accepted 29 December 2008
Available online xxx

Keywords:
Pseudomonas aeruginosa
Hyperoxia
Ventilator-associated pneumonia
Macrolide

ABSTRACT

Effects of hyperoxia on lethality in mice with *Pseudomonas aeruginosa* pneumonia were defined, and protective roles of macrolides were examined both in vitro and in vivo. Sub-lethal hyperoxia accelerated lethality of mice with *P. aeruginosa* pneumonia. Bacterial number was not different in the lungs, but higher in the liver of mice in hyperoxic conditions. Filter-sterilized culture supernatants of bacteria induced loss of viability of alveolar epithelial cells, which was exaggerated in hyperoxia. Metalloprotease blocking by inhibitor or gene-disruption in bacteria resulted in partial reduction of cytotoxic activity in culture supernatants. Co-culture of bacteria with sub-inhibitory concentrations of macrolides, such as azithromycin, reduced cytotoxic activity in the culture supernatants. Azithromycin provided significant survival benefit in hyperoxia–pneumonia model, which was associated with suppression of bacterial dissemination to extra-pulmonary organs. These results suggest that hyperoxia serves as an important cofactor for bacterial dissemination and lethality of *P. aeruginosa* pneumonia. Our data identify the potential of macrolides to protect individuals with *P. aeruginosa* pneumonia in the setting of hyperoxia.

1. Introduction

Ventilator-associated pneumonia (VAP) is a life-threatening infectious disease that causes substantial morbidity and mortality in respiratory and intensive care units of hospitals. Although oxygen supplementation is a critical supportive therapy for patients with severe hypoxemia, prolonged or even transient administration of oxygen may promote cellular damage and tissue injury [1,2]. Although mechanisms of oxygen toxicity to the lungs have not been carefully defined, it is likely that apoptosis and necrosis play a certain role in hyperoxia-associated lung injury [1,2]. Previously we have reported that hyperoxia exaggerates lethality and acute lung injury due to *Legionella pneumophila* in a mouse model of pneumonia [3]. In *Legionella* pneumonia, acceleration of apoptosis in the infected lungs without affecting bacterial number was demonstrated in the setting of hyperoxia. Although *Legionella* is a major cause of serious pneumonia requiring ventilator, more ubiquitous and antibiotic resistant organisms, such as methicillin-resistant *Staphylococcus aureus* and *Pseudomonas aeruginosa*, play a major part in etiology of VAP [4].

P. aeruginosa is an opportunistic pathogen that causes a wide range of acute and chronic infections, including sepsis, wound and pulmonary infection [5]. The recent epidemiological data demonstrated that *P. aeruginosa* is a leading cause of VAP, and pneumonia due to this pathogen is associated with extremely high rate of mortality, even when *P. aeruginosa* is isolated in relatively small numbers from the lungs [6,7]. *P. aeruginosa* is known to produce a variety of virulence factors, such as pigments, proteases and exotoxins [8]. These factors appear to contribute to injury of infected airway epithelial cells, which may cause disruption of barrier function of membrane and allow penetration of bacteria into the bloodstream [8]. However, which virulence factor is crucial for the development of VAP, or how hyperoxia modulates course and severity of VAP, remained to be elucidated.

After the first report of survival benefits of long-term macrolide treatment on chronic *P. aeruginosa* infection in diffuse

* Corresponding author. Tel.: +81 3 3762 4151x2396; fax: +81 3 5493 5415.
E-mail address: kazu@med.toho-u.ac.jp (K. Tateda).

1094-5539/$ – see front matter © 2008 Published by Elsevier Ltd.
doi:10.1016/j.pupt.2008.12.021

Please cite this article in press as: Kikuchi Y et al., Hyperoxia exaggerates bacterial dissemination and lethality in *Pseudomonas aeruginosa* pneumonia, Pulmonary Pharmacology & Therapeutics (2009), doi:10.1016/j.pupt.2008.12.021

panbronchiolitis patients [9,10], several investigators have reported efficacy of long-term macrolide therapy in cystic fibrosis and other forms of chronic pulmonary infections [11–13]. Although the exact mechanisms of macrolide efficacy are unknown, there are at least three possibilities, macrolide effects on bacteria at sub-inhibitory concentration (sub-minimum inhibitory concentration: sub-MIC), host defense systems, or both [14–16]. Several investigators including us have reported that macrolides at sub-MIC suppress major virulence factors of *P. aeruginosa*, such as pigment, exotoxin and exopolysaccharide [14,17,18].

In the present study, we examined effects of hyperoxia on lethality of mice with *P. aeruginosa* pneumonia, and dissemination of bacteria into distant organs. Also we explored protective roles of macrolides on pathogenesis of *P. aeruginosa* pneumonia in the setting of hyperoxia.

2. Materials and methods

2.1. Animal

Balb/c mice (Female, 6-week-old) were purchased from Charles River Japan. All mice were housed in the animal care facility at Toho University (Tokyo, Japan). All animal experiments were performed under the approval of animal center of Toho University (approval number: #169).

2.2. Construction of *aprA* or *lasB* deletion mutants from P. aeruginosa *PAO1*

P. aeruginosa PAO1 was used for the experiments. Elastase (*lasB*)- and alkaline protease gene (*aprA*)-deficient mutants were produced, as described previously [19,20]. Primers used for the PCR were shown in Table 1. Deficiency of these proteases was confirmed in ELISA using specific antibody [21].

2.3. Culture and inoculation of bacteria

P. aeruginosa was incubated on Mullar Hinton agar (Gibco, Grand Island, N.Y.) for overnight at 37 °C. Mice were anesthetized, and then 30 μl of bacterial suspension were administered intranasally [22].

Table 1
Primers for construction of *aprA* or *lasB* mutants.

Primer	Sequence (5′–3′)[a]	PCR step
For deletion of *aprA*		
AprA F1	CGCGCTAGCCGCTACGAGGTCGAGCAGAACCGC	1st round 5′, 2nd round 5′
AprA R1	cgcgcccgtgtcagcgcgTGCAGTTATCGGCCAGATCAGGCCG	1st round 3′
AprA F2	atctggccgataactgcaCGCGCTGACACGGGCGCG	1st round 5′
AprA R2	AGCAAGCTTCGAAGGCATGATCGCCAGCGTCCG	1st round 3′, 2nd round 3′
For deletion of *lasB*		
LasB F1	GAGGCTAGCGAGGCGCTGGCGCAGCTCAAGGAG	1st round 5′, 2nd round 5′
LasB R1	cggccgggaccaccgagcCAGGCCGAAGTACTCGGCCGACGC	1st round 3′
LasB F2	gccgagtacttcggcctgGCTCGGTGGTCCCGGCCGGCAC	1st round 5′
LasB R2	CCTAAGCTTTCCTACCGGCATTTCCGCATTCGCCGCG	1st round 3′, 2nd round 3′

[a] Underlined sequences and lower-case letters indicate the endonuclease restriction sites added for cloning into the plasmid pMT5059 and the sequences added for overlap-extention PCR, respectively.

2.4. Protease inhibitors used

The following protease inhibitors were purchased from Sigma-Aldrich: Pepstatin A, a potent inhibitor of acid proteases; AEBSF [4-(2-Aminoethyl)benzenesulfonyl fluoride hydrochloride], an irreversible serine protease inhibitor; E-64 [trans-epoxysuccinyl-L-leucylamino(4-guanidino)butane], an effective irreversible inhibitor of cystein protease; EDTA (Ethylenediaminetetraacetic acid), a potent inhibitor of metallopoteases.

2.5. Oxygen exposure to mice

Two hours after intranasal administration of bacteria, one group of mice was kept in hyperoxia for 60 h in an airtight chamber, whereas another group was placed in room air [3]. For hyperoxic exposure, the oxygen concentration in the chamber was kept at 90% by a regulated flow of oxygen, which was monitored with an in-line oxygen analyzer (model D2; Beckman, Fullerton, CA).

2.6. Lungs, blood and liver harvesting for analysis

After CO_2 asphyxia, the blood was collected by heart puncture, and 10 μl of a serial dilution of blood were inoculated on agar for determination of bacterial count. The lungs and liver were homogenized in 2 ml saline using a tissue homogenizer. Homogenates (10 μl) were inoculated on agar after serial 1:10 dilutions. The remaining homogenates were centrifuged at 2500 rpm for 10 min. The supernatants were passed through a 0.45 μm filter and stored at −20 °C until used.

2.7. Determination of caspase-3 and histone-associated DNA fragments in the lungs of mice infected with P. aeruginosa

To evaluate induction of apoptosis, levels of histone-associated DNA fragments and caspase-3 activity were determined in lung homogenates. DNA fragmentation was quantified by measuring histone-associated DNA fragments using an ELISA kit (Cell Death Detection ELISA^{plus}, Roche Diagnostics GmbH, Germany). Caspase-3 activity was determined by a colorimetric assay (R&D systems), in which caspase-specific peptide conjugated to the color reporter molecule *p*-nitroanilide was used. The data are expressed as a fold increase, comparing to those of control mice ($n = 5$).

2.8. Co-culture of bacteria with sub-MICs of macrolide

Bacteria were incubated in Muller Hinton broth at 37 °C for 48 h with or without sub-MICs of macrolides. The supernatants were prepared by centrifugation and filter-sterilization (0.2 μm), and then used for cell viability assay. The following macrolides were used in this study; azithromycin (AZM), erythromycin (EM), clarithromycin (CAM), oleandomycin (OL), josamycin (JM), rokitamycin (RKM), midecamycin (MDM), telithromycin (TEL). Previously, we have reported that effects of sub-MICs of macrolide on virulence factors and quorum-sensing molecules of *P. aeruginosa* PAO1 [23,24]. During these experiments, we have confirmed that 2 μg/ml of macrolides did not affect the bacterial number in test tube, although higher concentrations may suppress the growth of *P. aeruginosa* PAO1.

2.9. Cell culture, oxygen exposure and cell viability assay

The human lung alveolar epithelial cell line A549 was obtained from ATCC, and the cells were maintained in RPMI 1640 supplemented with 10% fetal calf serum (FBS). A549 cells were seeded to wells ($2–3 \times 10^4$ cells per well) in a 96-well plate. The cells were

Please cite this article in press as: Kikuchi Y et al., Hyperoxia exaggerates bacterial dissemination and lethality in *Pseudomonas aeruginosa* pneumonia, Pulmonary Pharmacology & Therapeutics (2009), doi:10.1016/j.pupt.2008.12.021

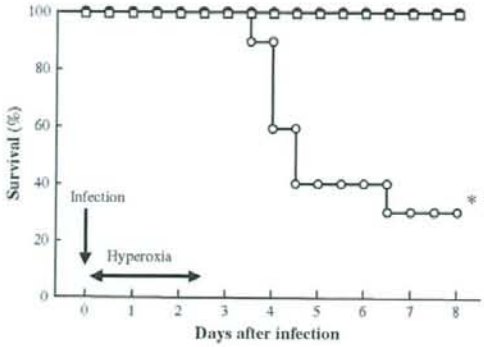

Fig. 1. Lethal sensitivity of mice with *P. aeruginosa* pneumonia in the setting of hyperoxia. Balb/c mice were intranasally inoculated with *P. aeruginosa* (6×10^6 CFU/mouse). One group (●) was kept in room air, whereas another group (○) was placed under hyperoxic conditions for 60 h, and then survival was observed in room air 8 days after bacterial challenge ($n = 10$). No death of mice was observed in hyperoxia alone without infection (□). *$P < 0.01$, compared with room air control group.

incubated in chamber of 5% CO_2 or 5% CO_2 plus 90% O_2 (ASTEC, Ltd., ACL-165D/ACM-165D, Japan) at 37 °C for 12–24 h with or without bacterial culture supernatants at 5% of final concentration. Cell viability was examined using the MTT assay using TetraColor ONE (Seikagaku Kogyo, Tokyo, Japan).

2.10. Statistical analysis

Statistical significance was determined using the unpaired, two-tailed alternate student's *t*-test. Survival curves were constructed by the Kaplan–Meier method, and were analyzed by logrank test. A significant difference was considered to be $P < 0.05$.

3. Results

3.1. Lethal sensitivity of mice with P. aeruginosa pneumonia in the setting of hyperoxia

As shown in Fig. 1, hyperoxia significantly exaggerated lethality of mice with *P. aeruginosa* pneumonia ($P < 0.01$). By 7 days after infection, approximately 70% of mice died under hyperoxia, whereas no death was observed in either infection in normoxic conditions or hyperoxia alone without infection. These data demonstrated that sub-lethal hyperoxia may potentiate lethality in *P. aeruginosa* pneumonia.

3.2. Bacterial number in the lungs and liver of infected mice under hyperoxia

We next examined bacterial number in the infected lungs and liver on day 1. As shown in Fig. 2, no difference in bacterial burden was observed in the lungs of mice exposed to hyperoxia as compared to animals maintained in room-air conditions. In contrast, drastic difference of bacterial number was observed in the liver. *P. aeruginosa* CFU in the liver of infected mice kept in room air was below the detection limit, whereas the liver of the hyperoxia group contained bacteria at a concentration of $>10^3$ CFU ($P < 0.01$). In blood, 2 of 7 mice (28.6%) were positive in *P. aeruginosa* in room-air group (mean bacterial number: 100 cfu/ml), whereas 3 of 5 mice (60.0%) were complicated with bacteremia in hyperoxia group (mean bacterial number: 133 cfu/ml). These data suggest that hyperoxia exaggerates dissemination of bacteria to extra-pulmonary organ liver, probably through bloodstream.

3.3. Caspase-3 and histone-associated DNA fragments in the lungs of mice infected with P. aeruginosa

After the induction of *P. aeruginosa* pneumonia, mice were kept in room air or hyperoxic condition for 1 day, and then caspase-3 activity and histone-associated DNA fragments in the lungs of mice were examined. As shown in Table 2, *P. aeruginosa* infection induced increase of caspase-3 activity in the lungs of mice kept in room air to approximately 180% of the control. Importantly, caspase-3 activity of the infected lungs of mice kept in hyperoxia did not differ from those of mice kept in room air. Although slightly higher values were observed in hyperoxia group in histone-associated DNA fragments, it was not statistically significant. These data demonstrated that hyperoxia is not likely to exaggerate apoptosis in the lungs of mice infected with *P. aeruginosa*, judging from apoptosis makers, such as caspase-3 and histone-associated DNA fragments.

3.4. Effects of filter-sterilized culture supernatants on epithelial cells

Effects of bacterial culture supernatants on epithelial cells were examined in an in vitro cell culture system. The

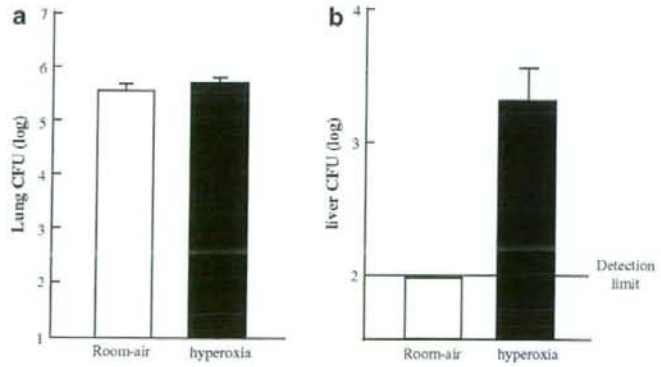

Fig. 2. Bacterial number in the lungs and liver of mice with *P. aeruginosa* pneumonia under hyperoxia. Balb/c mice were intranasally inoculated with *P. aeruginosa*. Then, one group was kept in room air (open column), whereas another group was placed under hyperoxic condition (closed column). The bacterial burden in the lungs and liver was assessed on day 1 post-infection ($n = 5$). *$P < 0.01$, compared with room air control group.

Please cite this article in press as: Kikuchi Y et al., Hyperoxia exaggerates bacterial dissemination and lethality in *Pseudomonas aeruginosa* pneumonia, Pulmonary Pharmacology & Therapeutics (2009), doi:10.1016/j.pupt.2008.12.021

Table 2
Caspase-3 and histone-associated DNA fragments in the lungs of infected mice kept in room air or hyperoxia.

Factors examined	Condition kept	Mean ± SD
Caspase-3	Room air	1.79 ± 0.44
	Hyperoxia	1.50 ± 0.40
Histone-DNA	Room air	64.6 ± 7.1
	Hyperoxia	73.5 ± 14.2

Mice were infected with *P. aeruginosa* and then kept in room air or hyperoxia. On day 1 after infection, caspase-3 and histone-associated DNA fragments in the lungs were examined ($n = 5$), and the results were expressed as fold increase of the control (no infection).

supernatants were prepared by centrifugation and filter-sterilization of culture supernatants of *P. aeruginosa*. Human alveolar epithelial cells (A549) were incubated with culture supernatants for 8 h, and change of morphology was examined. As shown in Fig. 3a, drastic alterations of cellular morphology, such as rounding, aggregation and detachment, were observed in a concentration-dependent manner. Next, we examined changes of cell viability in the presence of various concentrations of culture supernatants for 48 h in the setting of normoxia (21% O_2) or hyperoxia (90% O_2). Addition of culture supernatants decreased cell viability in a concentration-dependent manner under normoxia and hyperoxia. Especially, in the setting of hyperoxia, significantly higher reduction of cell viability was observed in 0.62–2.5% of culture supernatants, comparing to those in normoxia (Fig. 3b, $P < 0.01$). These results suggested that a high concentration of oxygen exaggerates epithelial cell damage by culture supernatants of *P. aeruginosa*.

3.5. Effect of protease inhibitors on cell viability in the presence of culture supernatants

Morphological changes of cells, such as rounding and detachment, prompted us to examine the contribution of bacterial proteases in culture supernatants, as it is known that *P. aeruginosa* produces several proteases. We examined effects of protease inhibitors Pepstatin A (acid proteases inhibitor), AEBSF (serine proteases inhibitor), E-64 (cysteine proteases inhibitor), EDTA (metalloproteases inhibitor) on cell viability in the presence of culture supernatant (5%) for 48 h under hyperoxia (Fig. 4). No protective effects of Pepstatin A, AEBSF or E-64 were observed in concentrations examined. On the other hand, the metalloprotease inhibitor EDTA significantly reduced loss of viability of epithelial cells at concentrations of 250 and 500 μM ($P < 0.05$).

3.6. Effects of deletion of *lasB*- or *aprA*-gene in P. aeruginosa on cytotoxic activity in the setting of hyperoxia

Next, we examined production of cytotoxic virulence factors in culture supernatants of *lasB*- or *aprA*-deficient isogenic mutants (Fig. 5). The culture supernatants (5%) of *P. aeruginosa* PAO1 parent strain induced reduction of viability of epithelial cells to approximately 50% of the control (no treatment). Although the restoration of viability was partial and modest, the deletion of *lasB*- or *aprA*-gene in *P. aeruginosa* reduced cytotoxic activity in culture supernatants from these strains. The data also suggested that alkaline metalloprotease (*aprA*) play more important role in cytotoxic activity than elastase (*lasB*) in *P. aeruginosa* PAO1 in the setting of hyperoxia.

3.7. Effects of co-culture with macrolide antibiotics on production of cytotoxic virulence factors by P. aeruginosa

P. aeruginosa was grown in the presence or absence of sub-MICs of macrolides, and then the culture supernatants were examined for their cytotoxic activities. A549 cells were incubated with 5% of culture supernatants for 48 h in the setting of hyperoxia, and then

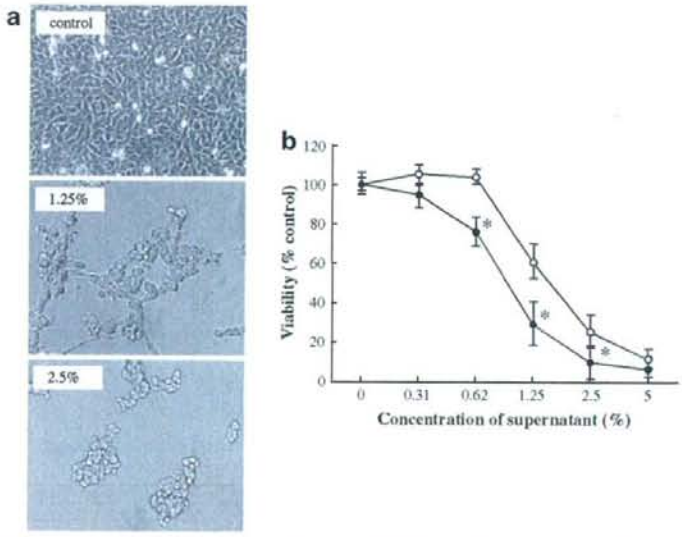

Fig. 3. Change of morphology and viability of epithelial cells in the presence of bacterial supernatants. a. A549 cells were incubated with filter-sterilized *P. aeruginosa* culture supernatant (0%, 1.25%, 2.5%) for 8 h in 5% CO_2 plus 90% O_2, and then the cell morphology was examined. b. A549 cells were incubated with various concentrations of culture supernatants for 48 h in 5% CO_2 plus 20% O_2 (ambient air) (○) or 5% CO_2 plus 90% O_2 (●), and then the cell viability was examined by MTT assay, as described in materials and methods. *$P < 0.01$, compared with 5% CO_2 group.

Please cite this article in press as: Kikuchi Y et al., Hyperoxia exaggerates bacterial dissemination and lethality in *Pseudomonas aeruginosa* pneumonia, Pulmonary Pharmacology & Therapeutics (2009), doi:10.1016/j.pupt.2008.12.021

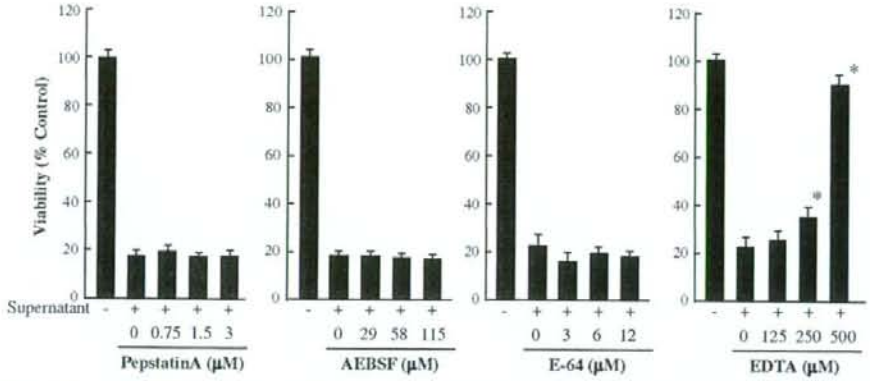

Fig. 4. Effect of protease inhibitors on induction of loss of cell viability by culture supernatants of *P. aeruginosa*. A549 cells were incubated with 5% of *P. aeruginosa* culture supernatant for 24 h in the presence of various concentrations of protease inhibitors under 5% CO_2 plus 90% O_2, and then the viability of cells was compared. *$P < 0.05$, compared with no protease inhibitor.

cell viability was compared. As shown in Fig. 6, AZM, TEL, CAM and EM suppressed production of cytotoxic virulence factors in a concentration-dependent manner. In contrast, JM, RKM, MDM and OL exhibited only subtle effects, even at a concentration of 10 μg/ml. From these experiments, we could not exclude effects of macrolide carried over on cell viability assay, although it seems unlikely because the expected final concentration of macrolides carry over was 0.125–0.5 μg/ml (20 times dilution of the supernatant).

3.8. Effects of AZM treatment on survival of mice with P. aeruginosa pneumonia in the setting of hyperoxia

AZM (30 mg/kg, PO) or control solvent was administered starting 2 days before infection for a total of 5 days, and *P. aeruginosa* was intranasally inoculated on day 0. The infected mice with or without AZM treatment were kept in 90% O_2 for 60 h, and then survival was monitored in room air for 10 days after infection (Fig. 7a). Infected mice exposed to hyperoxia started to die from day 4, with a final survival rate being approximately 50% by day 10. In contrast, no death of mice was observed in AZM treatment group ($P < 0.01$). These data suggest that AZM treatment is beneficial for *P. aeruginosa* pneumonia in the setting of hyperoxia.

3.9. Effects of AZM treatment on bacterial number in the lungs and liver

We examined bacterial number in the lungs and liver of mice 1 day after the infection. Administration of AZM and treatment of hyperoxia were performed as described in Fig. 7a. In the lungs, bacterial numbers were 4.5×10^5 and 2.5×10^4 cfu/lung for the control and AZM treatment group, respectively (Fig. 7b). Interestingly, bacteria were not detected in the liver of mice with AZM treatment group, whereas approximately 10^4 cfu/liver of *P. aeruginosa* was present in the control mice. These data demonstrated that

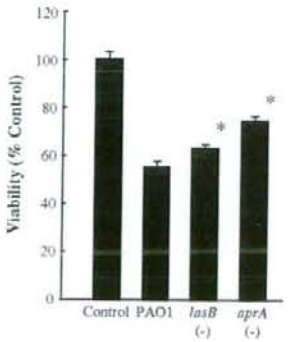

Fig. 5. Cytotoxic activities in culture supernatants of *lasB*- or *aprA*-deficient mutants. Cytotoxic activities in culture supernatants (5%) of *lasB*- or *aprA*-deficient mutants were compared to that of parent strain *P. aeruginosa* PAO1 in the setting of hyperoxia. *$P < 0.05$, compared with *P. aeruginosa* PAO1.

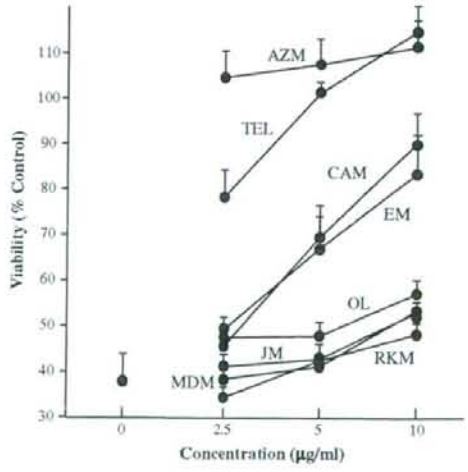

Fig. 6. Effects of co-culture with macrolide antibiotics on production of cytotoxic virulence factors of *P. aeruginosa*. *P. aeruginosa* PAO1 was incubated with 2.5, 5, 10 μg/ml of macrolide antibiotics at 37 °C for 24 h, and then the culture supernatants were prepared by centrifugation and filter-sterilization. A549 cells were incubated with 5% of the culture supernatants for 48 h in the setting of 5% CO_2 plus 90% O_2, and then the cell viability was compared.

Please cite this article in press as: Kikuchi Y et al., Hyperoxia exaggerates bacterial dissemination and lethality in *Pseudomonas aeruginosa* pneumonia, Pulmonary Pharmacology & Therapeutics (2009), doi:10.1016/j.pupt.2008.12.021

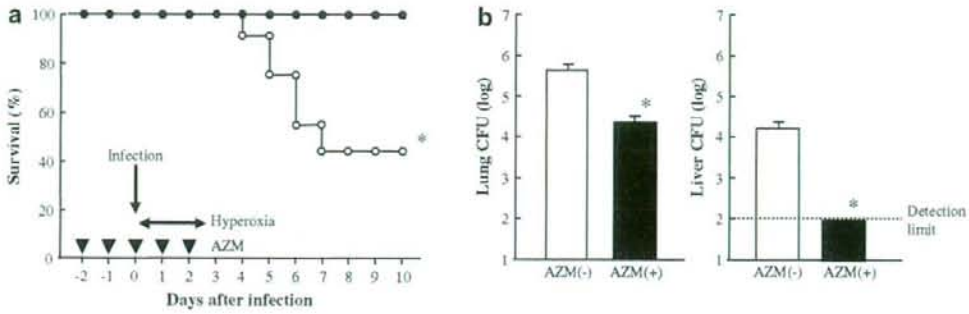

Fig. 7. AZM effects on bacterial number and survival of mice with *P. aeruginosa* pneumonia in the setting of hyperoxia. a. AZM (30 mg/kg, PO) (●) or control solvent (○) was administered from 2 days before infection for 5 days, and *P. aeruginosa* PAO1 was intranasally inoculated on day 0. The infected mice with or without AZM treatment were kept in 90% O_2 for 60 h, and then survival was monitored in room air for twice a day for 10 days after infection. b. AZM (30 mg/kg, PO) or control solvent was administered from 2 days before infection for 3 days, and *P. aeruginosa* PAO1 was intranasally inoculated on day 0. The infected mice with (closed column) or without AZM treatment (open column) were kept in 90% O_2 for 24 h, and then the bacterial number in the lungs and liver was examined ($n = 5$). *$P < 0.01$, compared with no treatment group.

AZM treatment reduced bacterial burden in the lungs and dissemination of bacteria to the liver in the setting of hyperoxia.

4. Discussion

The present study demonstrates that sub-lethal treatment of oxygen exaggerates *P. aeruginosa* pulmonary infection. Our data showed significantly higher bacterial burden in the liver, but not in the lungs, indicating development of bacterial dissemination in the setting of hyperoxia. The data obtained from protease blocking experiments and specific gene-disrupted mutants suggested involvement of metalloproteases, especially alkaline protease, for epithelial cell damage in the setting of hyperoxia. Importantly, this cytotoxic activity observed in culture supernatants was substantially abrogated when the bacteria were co-cultured with sub-MICs of AZM, TEL, EM and CAM. Consistent with these data, AZM treatment provided survival benefit in hyperoxia–pneumonia model. Collectively, these data suggest that hyperoxia may be an important cofactor for pathogenesis of *P. aeruginosa* pneumonia, and certain macrolides may be a therapeutic option for these individuals.

Previously, we have reported that hyperoxia lethally sensitized mice to *L. pneumophila* in a mouse model of pneumonia [3]. In the *Legionella* experiment, the mechanisms of exaggerated death of mice in the setting of hyperoxia were speculated to be an accelerated apoptosis in pulmonary cells and acute lung injury. In addition, no changes of bacterial burden were observed not only in the lungs, but also in the distant organs, liver and spleen. In the present study, pulmonary apoptosis markers, such as caspase-3 and histone-associated DNA fragments, were not different in *P. aeruginosa* pneumonia between the room air and hyperoxia groups, while significantly higher bacterial burden was observed in the liver of infected mice under hyperoxia. Although a clear mechanism to explain the difference between *Legionella* and *P. aeruginosa* infection is still unknown, these data suggested a minimum contribution of apoptosis in the lungs for hyperoxia-mediated high lethality in *P. aeruginosa* pneumonia model.

Alkaline protease and elastase are major extracellular virulence factors of *P. aeruginosa* [8,25]. These metalloproteases exhibit strong proteolytic activities for cells and tissues, including fibrin and elastin. It has been demonstrated that these enzymes induce rupture of tight-junction of epithelium and increase of permeability, which may be associated with tissue invasion and spreading of bacteria to distant organs [26,27]. Although the present data indicated a role of metalloproteases in cytotoxic activity in *P. aeruginosa*, those contributions appear to be partial. Conversely, these data suggested an involvement of other and/or unknown virulence factors for cytotoxic activity in culture supernatants of *P. aeruginosa*. In this regard, Marquart and associates recently found that *P. aeruginosa* produces a novel secreted protease (*P. aeruginosa* small protease; PASP), which exerts strong proteolytic activity in cornea [28]. Also, it is possible that multiple virulence factors may function additively or synergistically, as Azghani and colleagues have reported complementary actions of elastase and exotoxin A in disruption of epithelial barrier function and bacterial translocation [29].

Although hyperoxia promoted the *P. aeruginosa* culture supernatant-induced cell death of A549 cell, the difference between 5% CO_2 and 5% CO_2 plus 90% O_2 seems to be slight. It looks like that the results obtained from A549 cells could not explain the whole mechanisms of exaggerated lethality under hyperoxia. In vivo pneumonia model may include multiple factors, such as inflammatory cells recruited and production of oxygen-scavenger substances.

Efficacy of certain macrolides against chronic *P. aeruginosa* infection has been confirmed in several clinical settings, including cystic fibrosis and diffuse panbronchiolitis, although the exact mechanisms of actions are still unknown. Several investigators have reported macrolide effects on host immunological responses, bacterial virulence factor expression, or both [14–16]. We have previously reported sub-MIC macrolide effects on *P. aeruginosa*, such as suppression of virulence factors (pigment, protease and extotoxin A) [23], quorum-sensing systems [24], alterations in cell surface structures and exposure time-dependent bactericidal activity [18]. The present results are substantially consistent with previous reports, and further demonstrated protective roles of macrolides in epithelial cell damages by culture supernatants. Also, we observed that AZM treatment reduced bacterial burden in the lungs and liver, and provided survival benefits in *P. aeruginosa* pneumonia in the setting of hyperoxia. Although the exact mechanisms are unknown in *P. aeruginosa* clearance by AZM, it may be possible that AZM-exposed bacteria became less virulent and readily cleared. To this end, Giamarellos-Bourboulis and associates have reported efficacy of CAM in sepsis and VAP patients, in which acceleration of resolution of VAP and weaning from mechanical ventilation were demonstrated, although the mortality rate at day 28 was not altered [30]. Further research regarding the mechanisms of macrolide actions on bacteria, particularly metalloprotease-suppressing activity, in addition to clinical usefulness of

Please cite this article in press as: Kikuchi Y et al., Hyperoxia exaggerates bacterial dissemination and lethality in *Pseudomonas aeruginosa* pneumonia, Pulmonary Pharmacology & Therapeutics (2009), doi:10.1016/j.pupt.2008.12.021

macrolides, is warranted to prevent and treat a life-threatening *P. aeruginosa* infection, including VAP.

Acknowledgements

We thank Soichiro Kimura and Yoshikazu Ishii for their helpful discussion and Barbara H. Iglewski for a kind gift of *P. aeruginosa* PAO1. This work was supported by the Naito Foundation and grants from the Ministry of Education, Culture, Sports, Science and Technology of Japan.

References

[1] Waxman AB, Einarsson O, Seres T, Knickelbein RG, Warshaw JB, Johnston R, et al. Targeted lung expression of interleukin-11 enhances murine tolerance of 100% oxygen and diminishes hyperoxia-induced DNA fragmentation. J Clin Invest 1998;101:1970–82.

[2] Barazzone C, White CW. Mechanisms of cell injury and death in hyperoxia: role of cytokines and Bcl-2 family proteins. Am J Respir Cell Mol Biol 2000;22:517–9.

[3] Tateda K, Deng JC, Moore TA, Newstead MW, Paine 3rd R, Kobayashi N, et al. Hyperoxia mediates acute lung injury and increased lethality in murine *Legionella* pneumonia: the role of apoptosis. J Immunol 2003;170:4209–16.

[4] Chastre J, Fagon JY. Ventilator-associated pneumonia. Am J Respir Crit Care Med 2002;165:867–903.

[5] Richards MJ, Edwards JR, Culver DH, Gaynes RP. Nosocomial infections in medical intensive care units in the United States. National Nosocomial Infections Surveillance System. Crit Care Med 1999;27:887–92.

[6] Chastre J, Fagon JY. Ventilator-associated pneumonia. Am J Respir Crit Care Med 2002;165:867–903.

[7] Shaw MJ. Ventilator-associated pneumonia. Curr Opin Pulm Med 2005;11:236–41.

[8] Sadikot RT, Blackwell TS, Christman JW, Prince AS. Pathogen-host interactions in *Pseudomonas aeruginosa* pneumonia. Am J Respir Crit Care Med 2005;171:1209–23.

[9] Kudoh S, Uetake T, Hagiwara K, Hirayama M, Hus LH, Kimura H, et al. Clinical effects of low-dose long-term erythromycin chemotherapy on diffuse panbronchiolitis. Nihon Kyobu Shikkan Gakkai Zasshi 1987;25:632–42.

[10] Kudoh S, Azuma A, Yamamoto M, Izumi T, Ando M. Improvement of survival in patients with diffuse panbronchiolitis treated with low-dose erythromycin. Am J Respir Crit Care Med 1998;157:1829–32.

[11] Jaffe A, Francis J, Rosenthal M, Bush A. Long-term azithromycin may improve lung function in children with cystic fibrosis. Lancet 1998;351:420.

[12] Equi A, Balfour-Lynn IM, Bush A, Rosenthal M. Long term azithromycin in children with cystic fibrosis: a randomised, placebo-controlled crossover trial. Lancet 2002;360:978–84.

[13] Saiman L, Marshall BC, Mayer-Hamblett N, Burns JL, Quittner AL, Cibene DA, et al. Azithromycin in patients with cystic fibrosis chronically infected with *Pseudomonas aeruginosa*: a randomized controlled trial. JAMA 2003;290:1749–56.

[14] Kita E, Sawaki M, Oku D, Hamuro A, Mikasa K, Konishi M, et al. Suppression of virulence factors of *Pseudomonas aeruginosa* by erythromycin. J Antimicrob Chemother 1991;27:273–84.

[15] Nguyen T, Louie SG, Beringer PM, Gill MA. Potential role of macrolide antibiotics in the management of cystic fibrosis lung disease. Curr Opin Pulm Med 2002;8:521–8.

[16] Amsden GW. Anti-inflammatory effects of macrolides – an underappreciated benefit in the treatment of community-acquired respiratory tract infections and chronic inflammatory pulmonary conditions? J Antimicrob Chemother 2005;55:10–21.

[17] Sakata K, Yajima H, Tanaka K, Sakamoto Y, Yamamoto K, Yoshida A, et al. Erythromycin inhibits the production of elastase by *Pseudomonas aeruginosa* without affecting its proliferation in vitro. Am Rev Respir Dis 1993;148:1061–5.

[18] Tateda K, Standiford TJ, Pechere JC, Yamaguchi K. Regulatory effects of macrolides on bacterial virulence: potential role as quorum-sensing inhibitors. Curr Pharm Des 2004;10:3055–65.

[19] Gotoh N, Tsujimoto H, Tsuda M, Okamoto K, Nomura A, Wada T, et al. Characterization of the MexC-MexD-OprJ multidrug efflux system in Delta-mexA-mexB-oprM mutants of *Pseudomonas aeruginosa*. Antimicrob Agents Chemother 1998;42:1938–43.

[20] Kuwayama H, Obara S, Morio T, Katoh M, Urushihara H, Tanaka Y. PCR-mediated generation of a gene disruption construct without the use of DNA ligase and plasmid vectors. Nucleic Acids Res 2002;30. E2.

[21] Shigematsu T, Fukushima J, Oyama M, Tsuda M, Kawamoto S, Okuda K. Iron-Mediated regulation of alkaline proteinase production in *Pseudomonas aeruginosa*. Microbiol Immunol 2001;45:579–90.

[22] Tateda K, Takashima K, Miyazaki H, Matsumoto T, Hatori T, Yamaguchi K. Noncompromised penicillin-resistant pneumococcal pneumonia CBA/J mouse model and comparative efficacies of antibiotics in this model. Antimicrob Agents Chemother 1996;40:1520–5.

[23] Hirakata Y, Kaku M, Mizukane R, Ishida K, Furuya N, Matsumoto T, et al. Potential effects of erythromycin on host defense systems and virulence of *Pseudomonas aeruginosa*. Antimicrob Agents Chemother 1992;36:1922–7.

[24] Tateda K, Comte R, Pechere JC, Köhler T, Yamaguchi K, Van Delden C. Azithromycin inhibits quorum sensing in *Pseudomonas aeruginosa*. Antimicrob Agents Chemother 2001;45:1930–3.

[25] Kipnis E, Sawa T, Wiener-Kronish J. Targeting mechanisms of *Pseudomonas aeruginosa* pathogenesis. Med Mal Infect 2006;36:78–91.

[26] Azghani AO, Connelly JC, Peterson BT, Gray LD, Collins ML, Johnson AR. Effects of *Pseudomonas aeruginosa* elastase on alveolar epithelial permeability in guinea pigs. Infect Immun 1990;58:433–8.

[27] Azghani AO, Gray LD, Johnson AR. A bacterial protease perturbs the paracellular barrier function of transporting epithelial monolayers in culture. Infect Immun 1993;61:2681–6.

[28] Marquart ME, Caballero AR, Chomnawang M, Thibodeaux BA, Twining SS, O'Callaghan RJ. Identification of a novel secreted protease from *Pseudomonas aeruginosa* that causes corneal erosions. Invest Ophthalmol Vis Sci 2005;46:3761–8.

[29] Azghani AO. *Pseudomonas aeruginosa* and epithelial permeability: role of virulence factors elastase and exotoxin A. Am J Respir Cell Mol Biol 1996;15:132–40.

[30] Giamarellos-Bourboulis EJ, Pechère JC, Routsi C, Plachouras D, Kollias S, Raftogiannis M, et al. Effect of clarithromycin in patients with sepsis and ventilator-associated pneumonia. Clin Infect Dis 2008;46:1157–64.

Please cite this article in press as: Kikuchi Y et al., Hyperoxia exaggerates bacterial dissemination and lethality in *Pseudomonas aeruginosa* pneumonia, Pulmonary Pharmacology & Therapeutics (2009), doi:10.1016/j.pupt.2008.12.021

JOURNAL OF CLINICAL ONCOLOGY

ORIGINAL REPORT

First-Line Gefitinib for Patients With Advanced Non–Small-Cell Lung Cancer Harboring Epidermal Growth Factor Receptor Mutations Without Indication for Chemotherapy

Akira Inoue, Kunihiko Kobayashi, Kazuhiro Usui, Makoto Maemondo, Soji Okinaga, Iwao Mikami, Masahiro Ando, Koichi Yamazaki, Yasuo Saijo, Akihiko Gemma, Hitoshi Miyazawa, Tomoaki Tanaka, Kenji Ikebuchi, Toshihiro Nukiwa, Satoshi Morita, and Koichi Hagiwara

From the Department of Respiratory Medicine, Saitama International Medical Center, Saitama Medical University, Hidaka City, Japan

Submitted June 23, 2008; accepted October 9, 2008; published online ahead of print at www.jco.org on Month XX, 2008

Written on behalf of the North East Japan Gefitinib Study Group

Supported by grant-in-aids from Japan Society for Promotion of Science and Japanese Foundation for the Multidisciplinary Treatment of Cancer

Authors' disclosures of potential conflicts of interest and author contributions are found at the end of this article.

Corresponding author: Kunihiko Kobayashi, MD, PhD, Department of Respiratory Medicine, Saitama International Medical Center, Saitama Medical University, 1397-1 Yamane, Hidaka City, 350-1298 Japan; e-mail: kobakuni@saitama-med.ac.jp

0732-183X/08/2799-1/$20.00

DOI: 10.1200/JCO.2008.18.7658

ABSTRACT

Purpose
This multicenter phase II study was undertaken to investigate the efficacy and feasibility of gefitinib for patients with advanced non–small-cell lung cancer (NSCLC) harboring epidermal growth factor receptor (*EGFR*) mutations without indication for chemotherapy as a result of poor performance status (PS).

Patients and Methods
Chemotherapy-naïve patients with poor PS (patients 20 to 74 years of age with Eastern Cooperative Oncology Group PS 3 to 4, 75 to 79 years of age with PS 2 to 4, and ≥ 80 years of age with PS 1 to 4) who had *EGFR* mutations examined by the peptide nucleic acid-locked nucleic acid polymerase chain reaction clamp method were enrolled and received gefitinib (250 mg/d) alone.

Results
Between February 2006 and May 2007, 30 patients with NSCLC and poor PS, including 22 patients with PS 3 to 4, were enrolled. The overall response rate was 66% (90% CI, 51% to 80%), and the disease control rate was 90%. PS improvement rate was 79% ($P < .00005$); in particular, 68% of the 22 patients improved from ≥ PS 3 at baseline to ≤ PS 1. The median progression-free survival, median survival time, and 1-year survival rate were 6.5 months, 17.8 months, and 63%, respectively. No treatment-related deaths were observed.

Conclusion
This is the first report indicating that *EGFR* mutation-positive patients with extremely poor PS benefit from first-line gefitinib. Because there previously has been no standard treatment for these patients with short life expectancy other than best supportive care, examination of *EGFR* mutations as a biomarker is recommended in this patient population.

J Clin Oncol 27. © 2008 by American Society of Clinical Oncology

INTRODUCTION

Lung cancer is the leading cause of cancer death worldwide, and approximately 80% of cases are non–small-cell lung cancer (NSCLC). Many patients with NSCLC have advanced disease at diagnosis and a poor prognosis. For patients with advanced NSCLC who are young and have a good performance status (PS), systemic chemotherapy, such as cisplatin plus gemcitabine or carboplatin plus paclitaxel, is administered as a standard treatment and has been shown to prolong their overall survival.[1,2] However, for patients with poor PS (generally ≥ PS 3), there is no standard treatment except best supportive care (BSC), and most die within 3 to 4 months.[2]

Gefitinib (Iressa; AstraZeneca, Wilmington, DE), an orally active, epidermal growth factor receptor (*EGFR*) tyrosine kinase inhibitor (TKI), has shown novel antitumor activity in patients with advanced NSCLC.[3,4] A recent large randomized trial proved noninferiority of gefitinib to docetaxel in the second- or third-line treatment of NSCLC,[5] although, when used in combination with standard chemotherapy, gefitinib failed to demonstrate efficacy in chemotherapy-naïve patients with advanced NSCLC.[6,7] Because the toxicity of gefitinib is less than that of cytotoxic agents, its utility as first-line treatment for patients with NSCLC having poor PS was studied. The previous study conducted in Japan suggested that gefitinib should not be used in unselected patients with poor PS due to low efficacy and

high toxicity, including interstitial lung disease.[8] However, this study was done at the time when the close relationship between some specific *EGFR* somatic mutations and the sensitivity to EGFR-TKI was unknown.

Two pivotal studies have revealed that somatic mutations of the *EGFR* gene in exons 18 to 21, which encode for the regions close to the adenosine triphosphate-binding pocket of the kinase domain, are associated with the response in patients treated with gefitinib.[9,10] Most of these mutations were observed in two hotspots: in-frame deletions, including amino acids at codons 746 to 750 (E746-A750) in exon 19, and an amino acid substitution at codon 858 (L858R) in exon 21, which is more frequent in patients with NSCLC in Asian countries but is also detected in those in Western countries.[11-13] In a prospective phase II trial of first-line gefitinib for patients with advanced NSCLC with such *EGFR* mutations, we have demonstrated a high response rate (75%) and long progression-free survival (PFS; 9.7 months).[14] Several other studies have supported this result, indicating that an EGFR-TKI provides a clinical benefit in selected patients with NSCLC,[15-19] although these studies enrolled only patients with PS 0 to 2. Some reports have described patients with NSCLC and poor PS who dramatically improved with gefitinib treatment,[20,21] but these reports were case studies.

We have developed the peptide nucleic acid (PNA)-locked nucleic acid (LNA) polymerase chain reaction (PCR) clamp method, a new technology to detect sensitive and insensitive *EGFR* mutations from both cytologic and tissue specimens[22] that has become available in clinical practice in Japan. This technique enabled us to assess the *EGFR* mutation status in patients with poor PS using specimens isolated by noninvasive procedures.[17,22,23] This led us to test our hypothesis that, for selected patients with NSCLC patients having *EGFR* mutations, gefitinib may be a salvage therapeutic option, even for patients in a poor condition who would not be candidates for standard chemotherapy.

In this context, we conducted this prospective phase II study to evaluate the efficacy and feasibility of first-line gefitinib for patients with NSCLC having extremely poor PS and harboring *EGFR* mutations.

PATIENTS AND METHODS

Patient Selection

This study was performed in accordance with the Helsinki Declaration (1964, amended in 2000) of the World Medical Association, and the protocol was approved by the institutional review board of each participating institution. The main eligibility criteria was to select chemotherapy-naive patients with NSCLC with both sensitive *EGFR* mutations and no indication for chemotherapy because of poor PS. Namely, patients having exon 19 deletions, L858R, L861Q, G719A, or G719S were included, but those with a resistant T790M mutation were excluded. Patients 20 to 74 years of age with Eastern Cooperative Oncology Group PS 3 to 4, those 75 to 79 years of age with PS 2 to 4, and those ≥ 80 years of age with PS 1 to 4 were eligible. Patients were also required to have estimated life expectancy of less than 4 months by BSC alone. Other eligibility requirements were stage IIIB to IV or postoperative recurrent NSCLC, presence of a measurable lesion according to the Response Evaluation Criteria in Solid Tumors criteria, adequate liver function (AST and ALT ≤ 100 U/L, total bilirubin < 2.0 mg/dL), and written informed consent. Oxygen therapy was permitted in cases of tumor progression.

EGFR *Mutation Analysis*

Cytologic specimens such as those obtained from sputum, bronchial washing, pleural effusion, and needle aspiration biopsy were divided into two samples. The first sample was used to confirm pathologically that cancer cells were present in the specimen. The second sample was subjected to an *EGFR* mutation test based on the PNA-LNA PCR clamp method. Briefly, genomic DNA fragments surrounding mutation hot spots of the *EGFR* gene are amplified by PCR in the presence of a clamp primer synthesized from PNA and with a wild-type sequence. This leads to the preferential amplification of the mutant sequence, which is detected by a fluorescent primer that incorporates LNA to increase the specificity. As a result, a mutant *EGFR* sequence is detected in the presence of a 100- to 1,000-fold wild-type sequence.[17,22,23] Thus by the PNA-LNA PCR clamp, a small number of *EGFR* mutation-positive cancer cells are detected within 3 hours. The sensitivity and specificity of the PNA-LNA PCR clamp were 97% and 100%, respectively.[23]

Four institutions routinely examined *EGFR* mutations by the PNA-LNA PCR clamp in our laboratory in Saitama Medical University as part of their clinical practice. Another nine institutions, where *EGFR* mutation testing was not routine, sent materials to the same laboratory after obtaining the informed consent for both testing *EGFR* mutations and the possibility to enter this study in the event of a mutation-positive result.

Drug Administration

Gefitinib (250 mg/d) was orally administered once daily. Patients continued uninterrupted treatment until they experienced disease progression or appearance of intolerable toxicity or until they withdrew consent. For patients with severe toxicity, the gefitinib dosing schedule could be modified to every second day. Second-line chemotherapy or other treatments after the termination of gefitinib therapy were permitted.

Treatment Assessment

We evaluated objective tumor responses as complete response, partial response, stable disease, or progressive disease in accordance with the Response Evaluation Criteria in Solid Tumors. Disease control was defined as the best response out of complete response, partial response, or stable disease, which was confirmed and sustained for 4 weeks or longer. Baseline assessments were performed within 28 days of treatment commencement. During treatment, assessments were performed every 4 weeks for the first 4 months and then every 8 weeks until disease progression. All adverse events were reported, and severity was graded by the National Cancer Institute Common Toxicity Criteria (version 3.0). Data were also collected when gefitinib treatment was interrupted or withdrawn due to adverse events. Routine clinical and laboratory assessments were performed at least every 4 weeks. PS was assessed according to Eastern Cooperative Oncology Group criteria.

Statistical Analyses

There has been little information available on an active treatment for patients with NSCLC having extremely poor PS. From our clinical experience, it seemed that gefitinib was effective in *EGFR* mutation-positive patients, even if their PS was poor. Therefore, we hypothesized that at least half of the poor PS patients would benefit from gefitinib if their tumor was positive for *EGFR* mutation. As the primary end point of this study, we used an overall response rate (ORR), defined as the proportion of patients in whom best response was a complete or partial response among all per-protocol patients. We assumed that an ORR of 75% in eligible patients would indicate potential clinical usefulness, whereas an ORR of 50% would be the lower limit of clinical usefulness, taking into account the retrospective studies of EGFR-TKI for patients with good PS.[24] On the basis of this assumption, our study was designed to have 95% power and had a .10 level of significance. The most informative secondary end point to clinicians was PS improvement rate, which was defined as the proportion of per-protocol patients whose PS during gefitinib treatment was improved from baseline. We also assumed that a PS improvement rate of 50% in eligible patients would be the lower limit of clinical usefulness. The other secondary end points were toxicity, PFS, and overall survival (OS). PFS was defined as the interval between the start of the treatment and the date of the first observation of disease progression or death from any cause. Patients who were alive without disease progression at the data cutoff point (April 30, 2008) were censored at the last point that the patients were assessed to be progression-free. PFS and OS were estimated by the Kaplan-Meier method, and the differences between subgroups were analyzed by log rank. *P* values less than .05 was considered to be significant.